Nanotubes and Nanodevices:

Theory and Simulation

Plato

427 - 347 BC, Athens, Greece

In his theory of Forms, Plato rejected the changeable, deceptive world that we are aware of through our senses proposing instead his world of ideas which were constant and true.

Ideal NT: Electronic Structure

b=0.14 nm

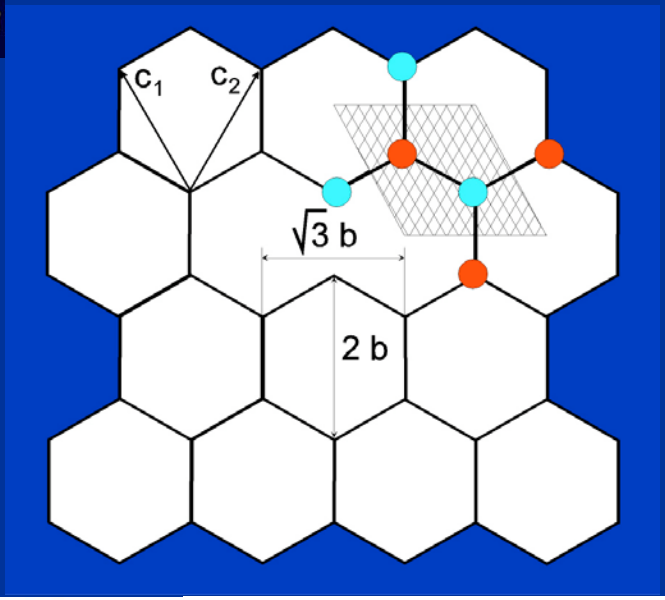

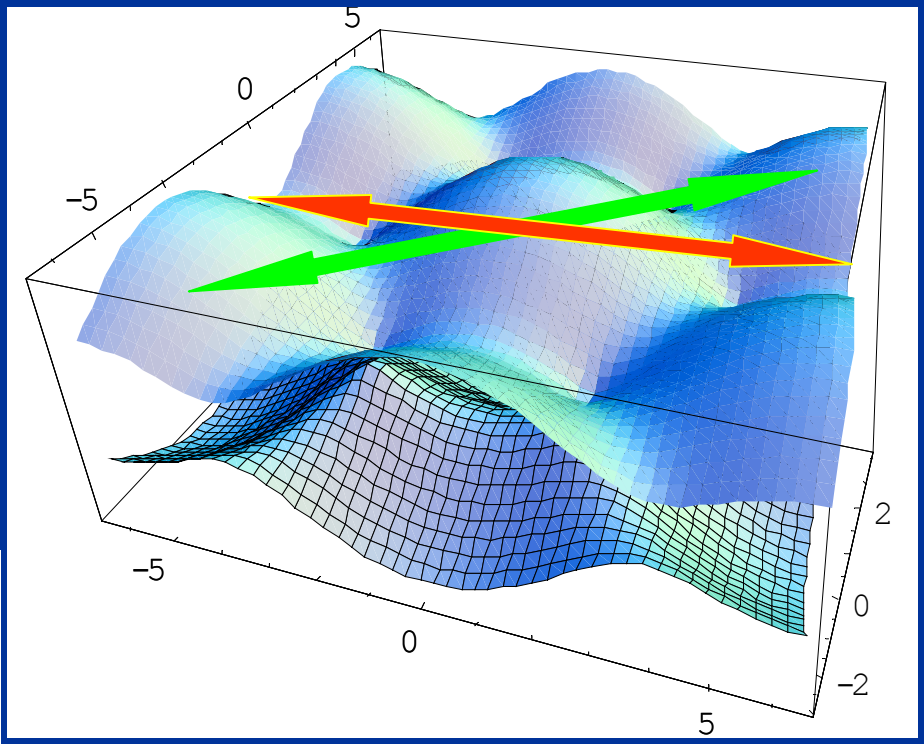

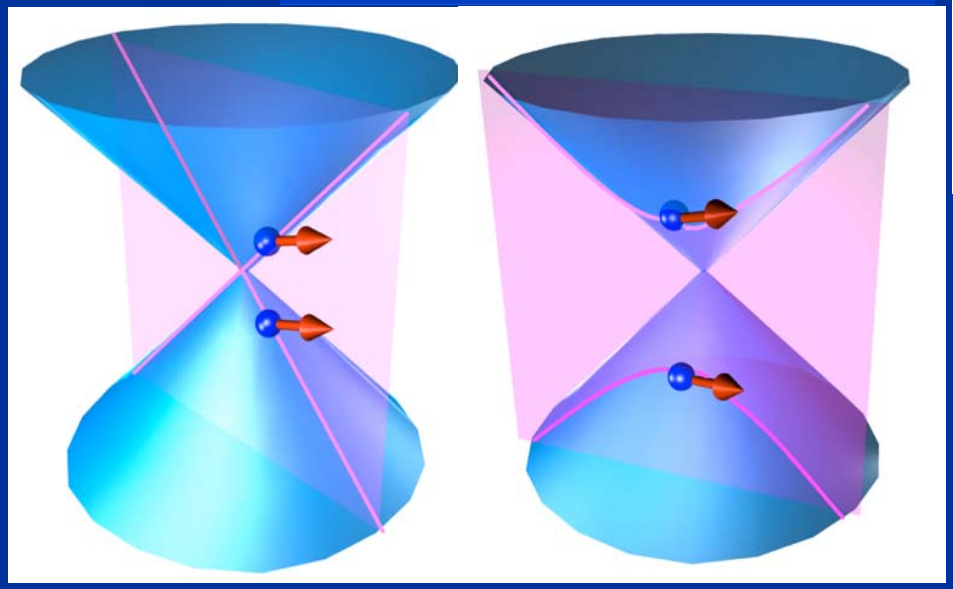

- Graphene = a monolayer of graphite is the zero-gap semiconductor
- 6 Fermi-points
- 2 special directions : Armchair and Zigzag (0° and 30° to diag.)

Ideal NT: Electronic Structure

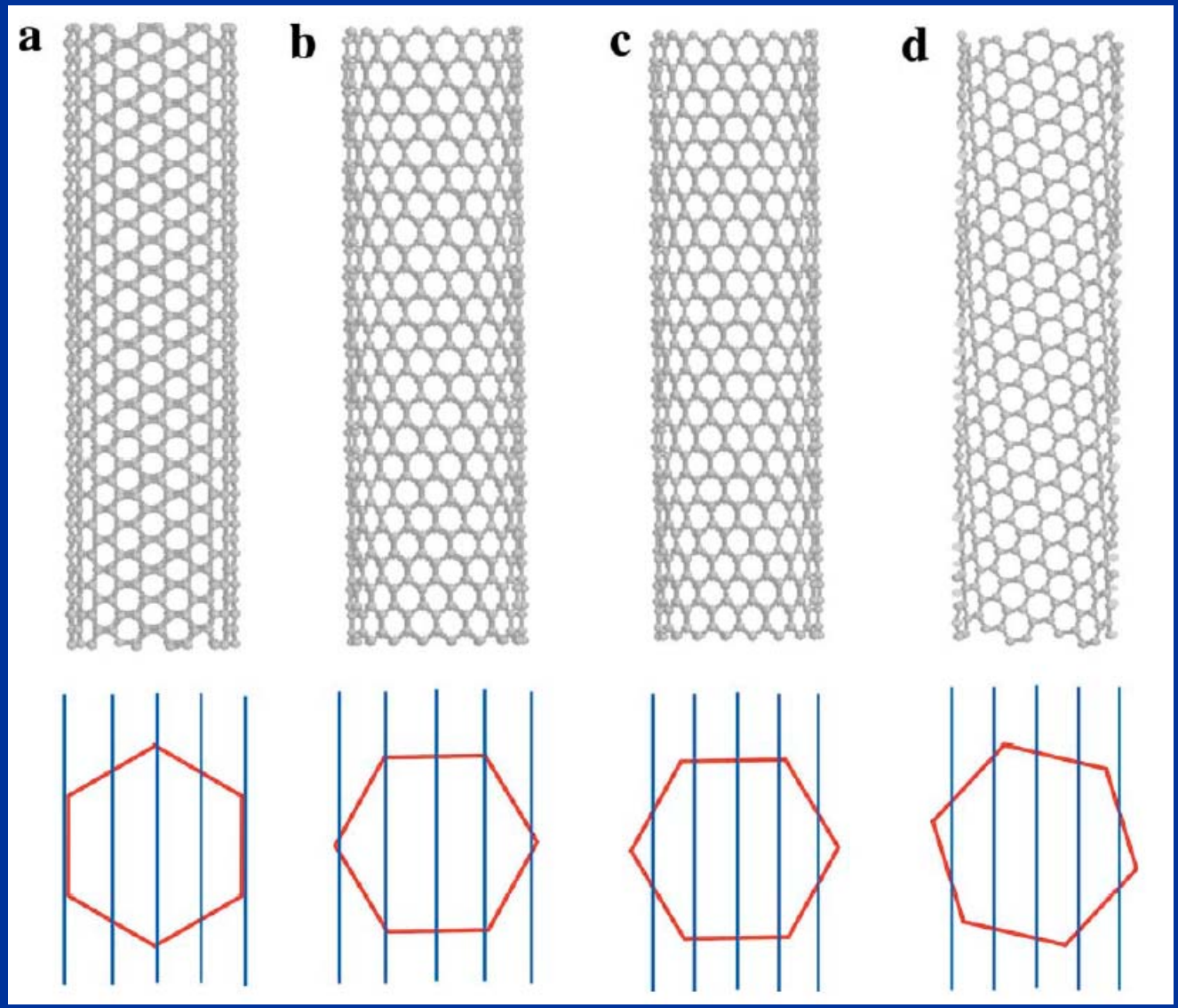

One-Electron Energy

- Scrolling impose quantization of transverse momentum k_t=<*integer*>/R
- Fermi-points (K and -K) are within band (A) or within energy gap (Z).
- Gap (energy scale) depends on $1/R_{NT}$.

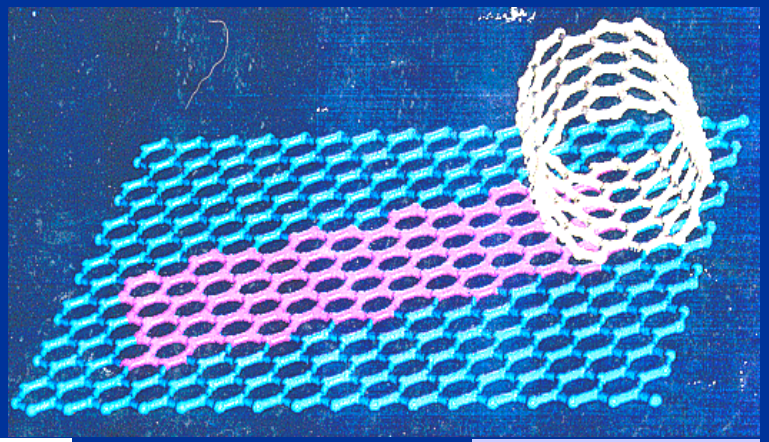

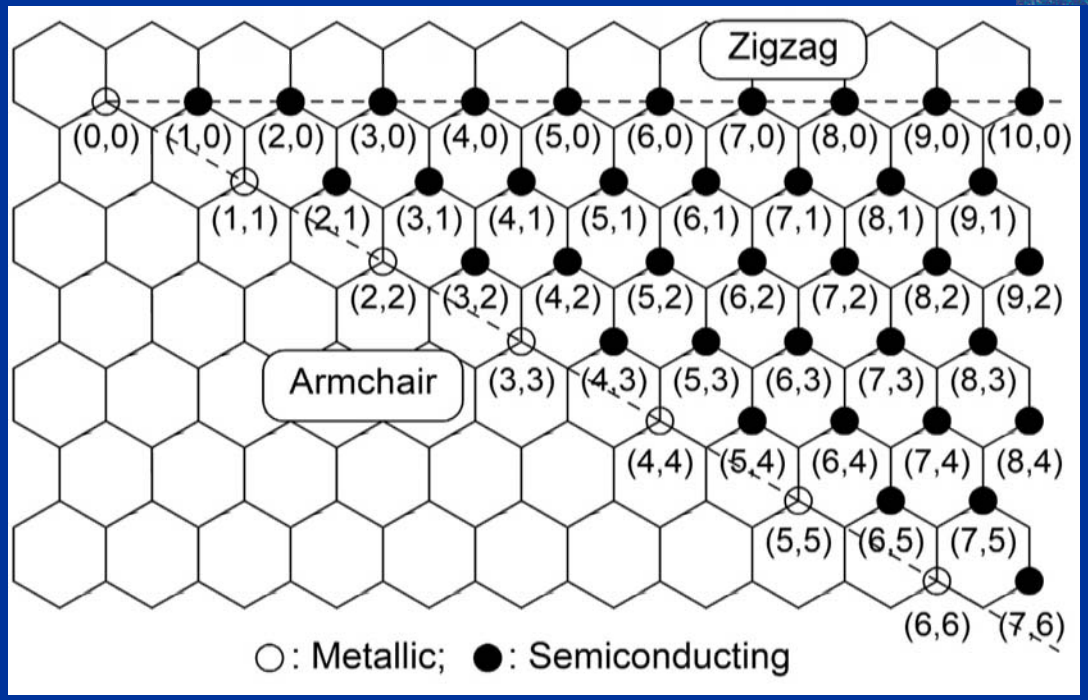

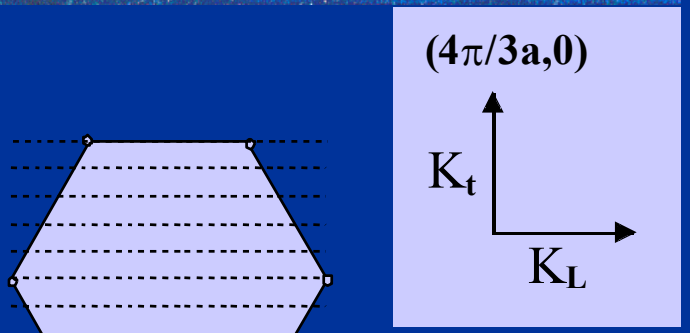

1/3 of SWNTs are "metallic"

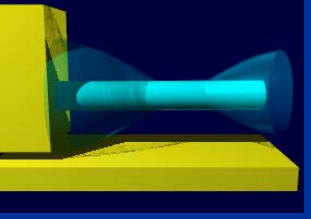

Electronic Structure (2)

- 2 special directions : Armchair and Zigzag (0° and 30° to diag.)
- Quantization results in 2 x n degenerate subbands, labeled with angular momentum, wavevector and pseudospin
- Gap depends on chirality;
- NT radius defines energy gap.

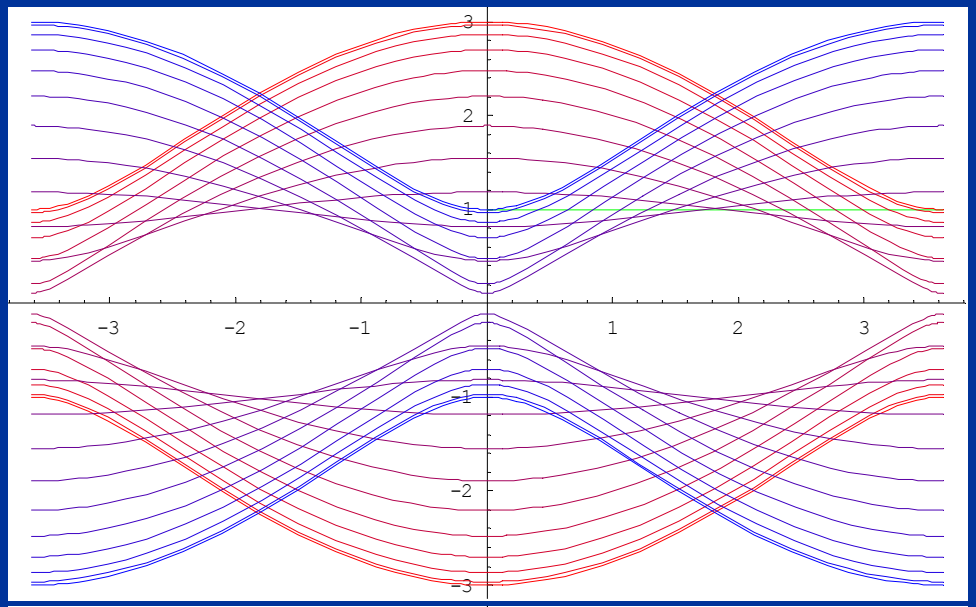

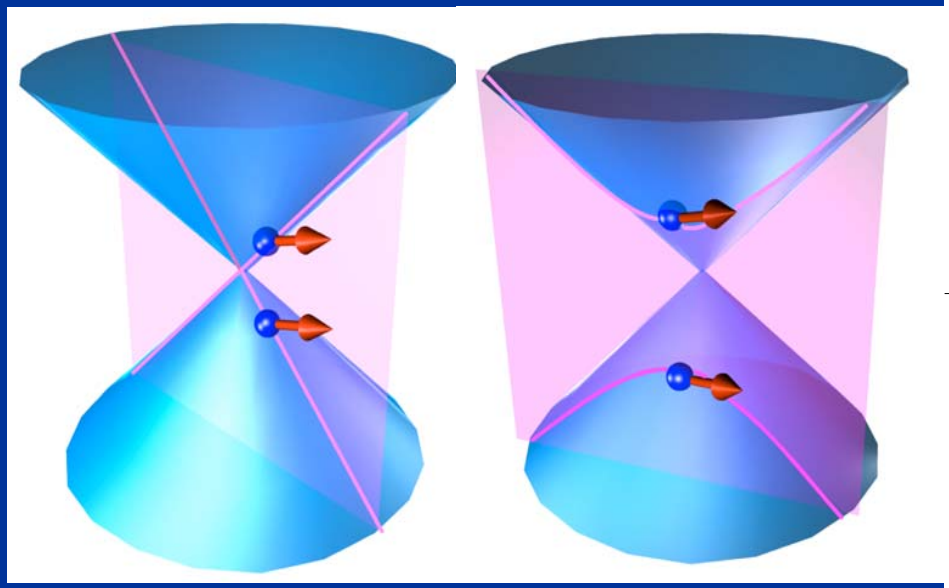

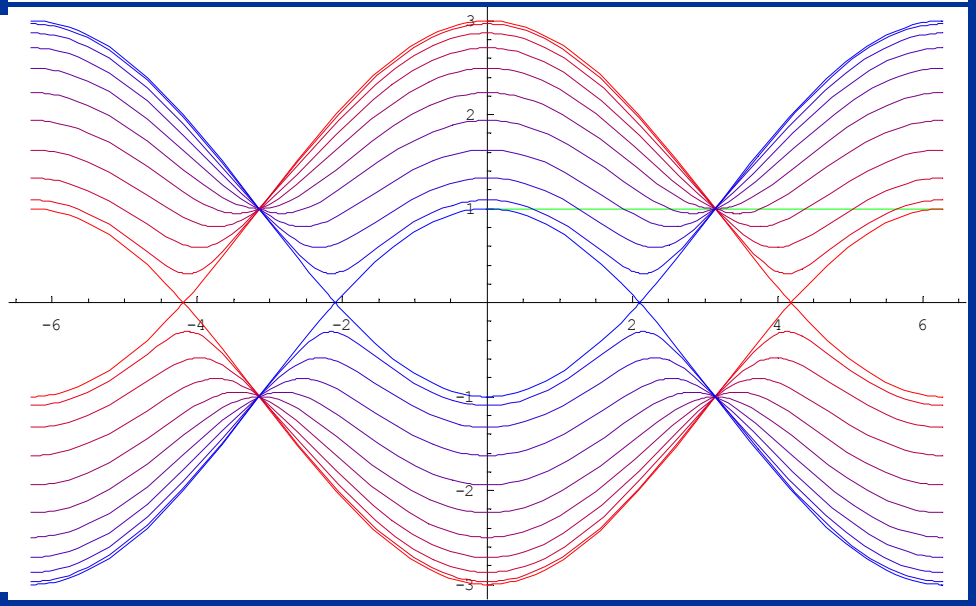

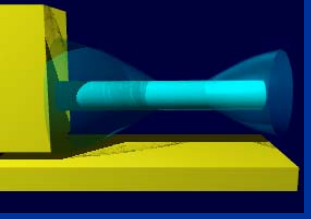

Electronic Structure (3)

$$\rho(\ell) = e\int_0^{E_o(\ell)} \nu(E)dE$$

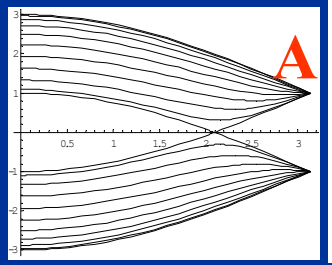

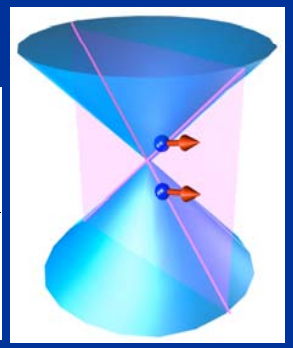

- **charge density follows LDOS and local chemical potential (or electric potential because E_F=const)**

$$E_o(\ell) = \Delta W - e\phi^{act}(\ell)$$

- **M-NT DOS=const**

$$\nu_M = \frac{8}{3\pi b\gamma_0}$$

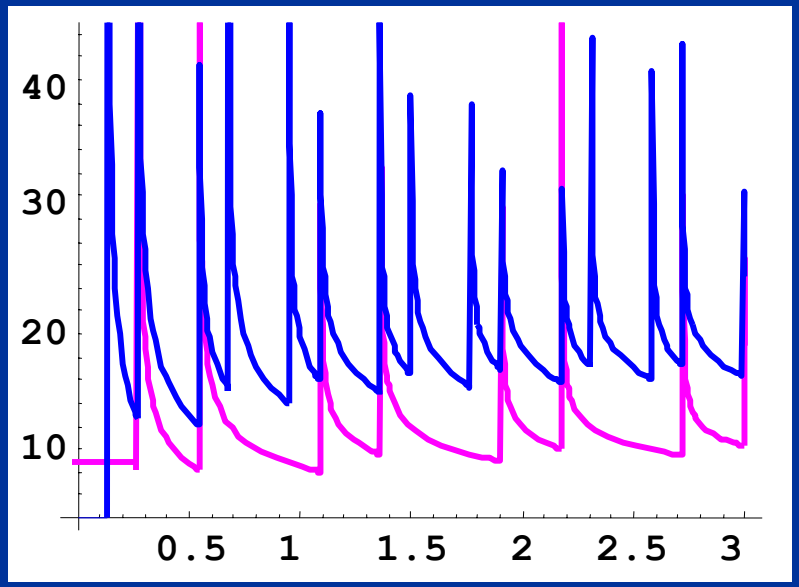

- **As a result a local connection holds between 1D charge and 1D potential**

$$\rho(\ell) = -e^2\nu_M\phi^{act}(\ell)$$

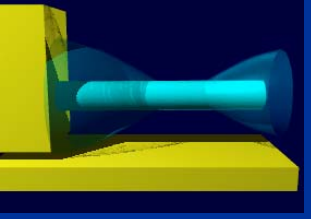

Poisson Equation in 1D

- Electric potential is divided in 2 parts:

$$\phi^{act}(\mathbf{r}) = \phi^{ext}(\mathbf{r}) + 4\pi \int G(\mathbf{r}, \mathbf{r}')\rho(\mathbf{r}')\mathbf{dr}'$$

- Integral equation for charge density

$$\frac{\rho(z)}{e^2 \nu_M} + \int_0^\infty F(z, z')\rho(z')dz' = -\phi^{ext}(z)$$

is reduced to 1D by substituting 1D Green function

$$F(z, z') = \frac{1}{4\pi^2} \int_{-\pi}^{\pi} \int_{-\pi}^{\pi} 4\pi G((z, R, \alpha), (z', R, \alpha'))d\alpha d\alpha'$$

1D Green function includes the charge and image charges (*i.e.* the geometry of the device)

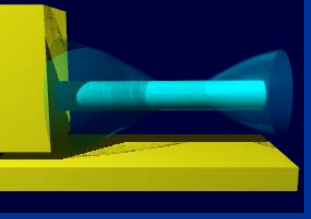

Poisson Equation in 1D (2)

1D Green function of device with a (close) gate has the form:

$$F(z,z') = \frac{2}{\pi\Delta z} K\left(-\frac{4R^2}{|\Delta z|^2}\right) - \frac{1}{\sqrt{(\Delta z)^2 + 4h^2}} \approx$$

Strong screening allows to cut the Coulomb potential which is under-screened in 1D in the opposite case

$$\approx \frac{1}{\pi R}\log\left(\frac{8R}{\Delta z}\right), \qquad \Delta z \ll R,$$

$$\approx \frac{1}{\Delta z}, \qquad R \ll \Delta z \ll 2h,$$

$$\approx \frac{2h^2}{(\Delta z)^3}, \qquad z \gg 2h$$

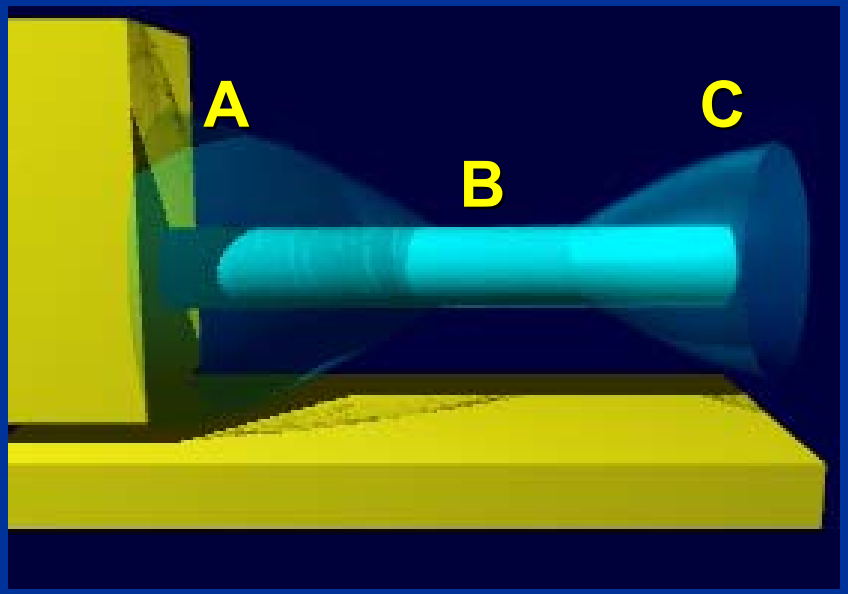

In a continuum electrostatics the NT device may be divided in three parts: A. screened root, B. main cantilever, C. underscreened tip

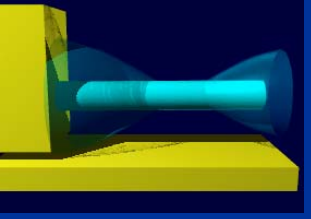

NT Electrostatics

- Linear connection between electric potential and a charge

$$\rho(z) \approx -c_\infty \phi^{ext}(z)$$

which fulfills exactly at a large separation from the contact region

$$\rho_\infty = -\phi_\infty^{ext} c_\infty$$

for a straight NT it gives an analytic solution in a closed form

where

$$c_\infty = \left(\frac{1}{e^2 \nu_M} + \frac{1}{c_\infty^{met}} \right)^{-1}$$

$$c_\infty^{met} = \left(\int_{-\infty}^{\infty} F(\Delta z) d\Delta z \right)^{-1} = \frac{1}{2 \log\left(\frac{2h}{R}\right)}$$

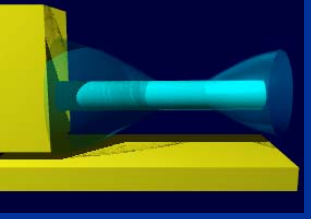

Poisson Equation in 1D (3)

- Formal solution in 1D Fourier Transform reads as:

$$\rho_k = -\frac{\phi_k^{ext}}{\frac{1}{e^2 \nu_M} + 2\pi F_{2k}}$$

- For our device geometry the Fourier Transform of 1D GF :

$$F_{2k} = \frac{1}{\pi}\left(I_0(kR)K_0(kR) - K_0(2hk)\right)$$

it decays with k.
Therefore, substitution of

$$F_{20} = \frac{1}{\pi}\log\left(\frac{2h}{R}\right)$$

gives a reasonable accuracy and allows analytical solution.

Poisson Equation in 1D (4)

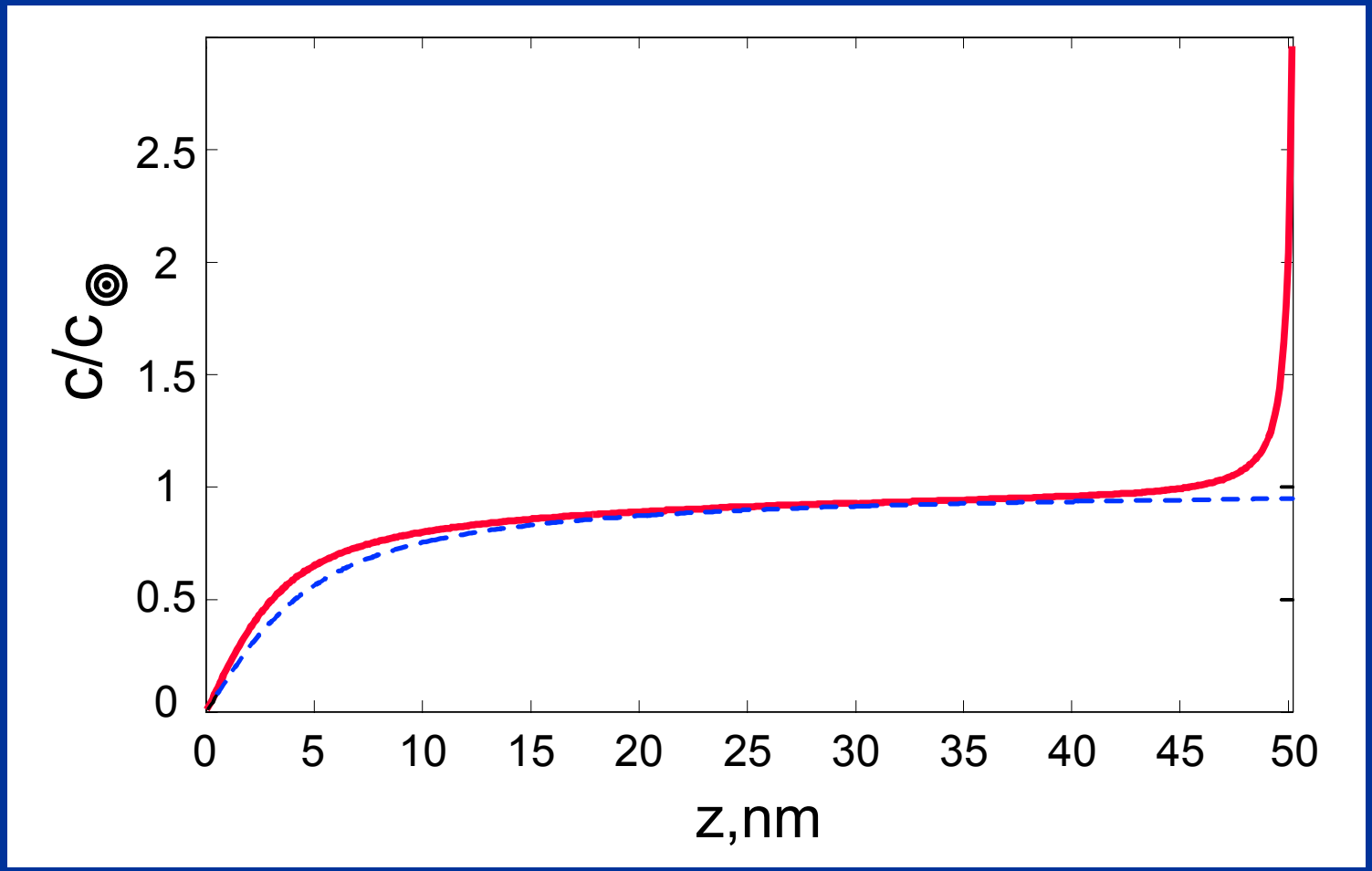

- Comparison of analytical approximation and exact solution of integral equation confirms the use of Continuum Compact Model for Nanotube Electrostatics

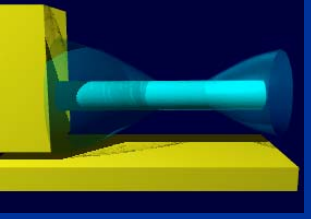

Quantum Capacitance

- Within our approximations, a NT device (charge density) is described by an atomistic capacitance which has two terms

$$\rho_\infty = -\frac{\varphi^{\mathrm{xt}}}{C_m^{-1} + C_A^{-1}} \simeq -\varphi^{\mathrm{xt}}\, C_m \left(1 - \frac{C_m}{C_A}\right)$$

- geometric capacitance (of a metallic cylinder)

and

- quantum capacitance

$$C_m^{-1} = 2\log\left(\frac{2h}{R}\right)$$

$$C_A^{-1} = \frac{1}{e^2 \nu_M}$$

- the quantum capacitance is analogous to QC proposed by S. Luriy in 1988 for 2DEG

$$C_{\mathrm{2DEG}}^{-1} = \frac{\pi\hbar^2}{m^* e^2} = \pi a_B^*$$

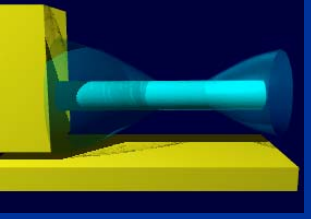

Solution for Distorted NT

- Similarly to a straight NT, the integral eq. for charge density reads as:

$$\frac{\rho(l)}{e^2\nu_M} + \int_0^L F(l,l')\rho(l')dl' = -\phi^{ext}(\mathbf{r}(l))$$

- Write a solution using a perturbation theory:

$$h = h_0 + \delta h \qquad F_1 = F_0 + \delta F \qquad \rho = \rho_0 + \delta\rho$$

- Some terms of equation

$$\frac{\delta\rho(z)}{e^2\nu_M} + \int_0^\infty F_0(z,z')\delta\rho(z')dz' = -\int_0^\infty \delta F(z,z')\rho_0(z')dz' - \frac{\partial\phi^{ext}}{\partial h}\,\delta h$$

can be represented as a capacitance of a metallic cylinder

$$c(z) \approx c^{met}(z)\left(1 - \frac{c^{met}(z)}{e^2\nu_M}\right)$$

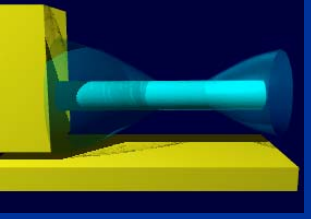

Shroedinger-Poisson vs. Boltzmann equation

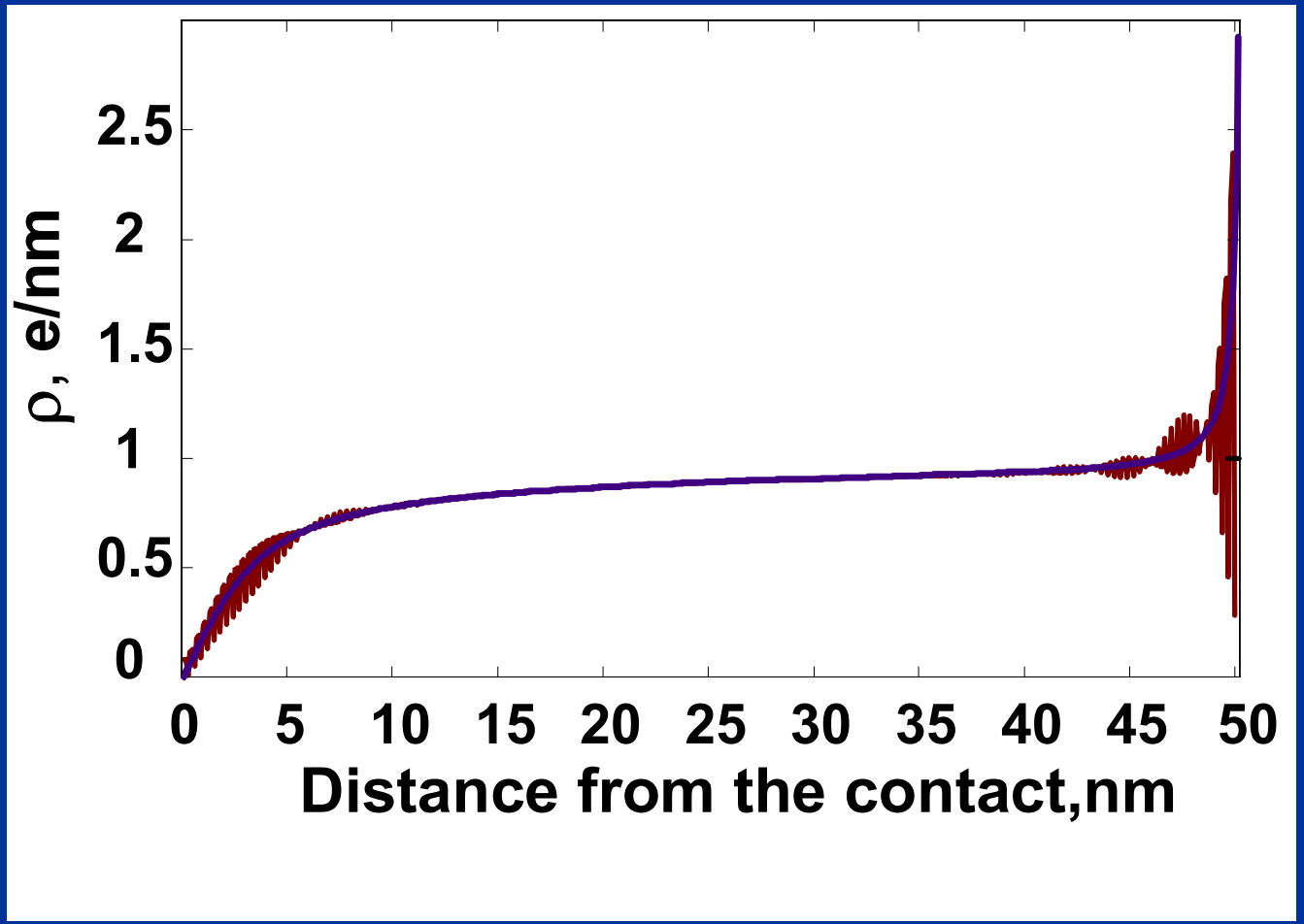

- Solution of selfconsistent Shroedinger-Poisson equation coincides with classic charge owing to high DOS of NT shell
- It gives a base for developing a Compact Device Model for SWNT Electrostatics

K.A.Bulashevich, S.V.Rotkin, "Nanotube Devices: Microscopic Model," JETP Letters 75 (4), 205 (2002)

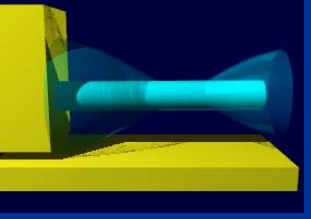

Atomistic view on E/S force

- Tight-binding (1SB) approximation was used for calculating the charge distribution with external potential applied to NT device
- Finite size effects are clearly seen: Quantum Beating at the NT ends
- Besides that QM results agrees with BP

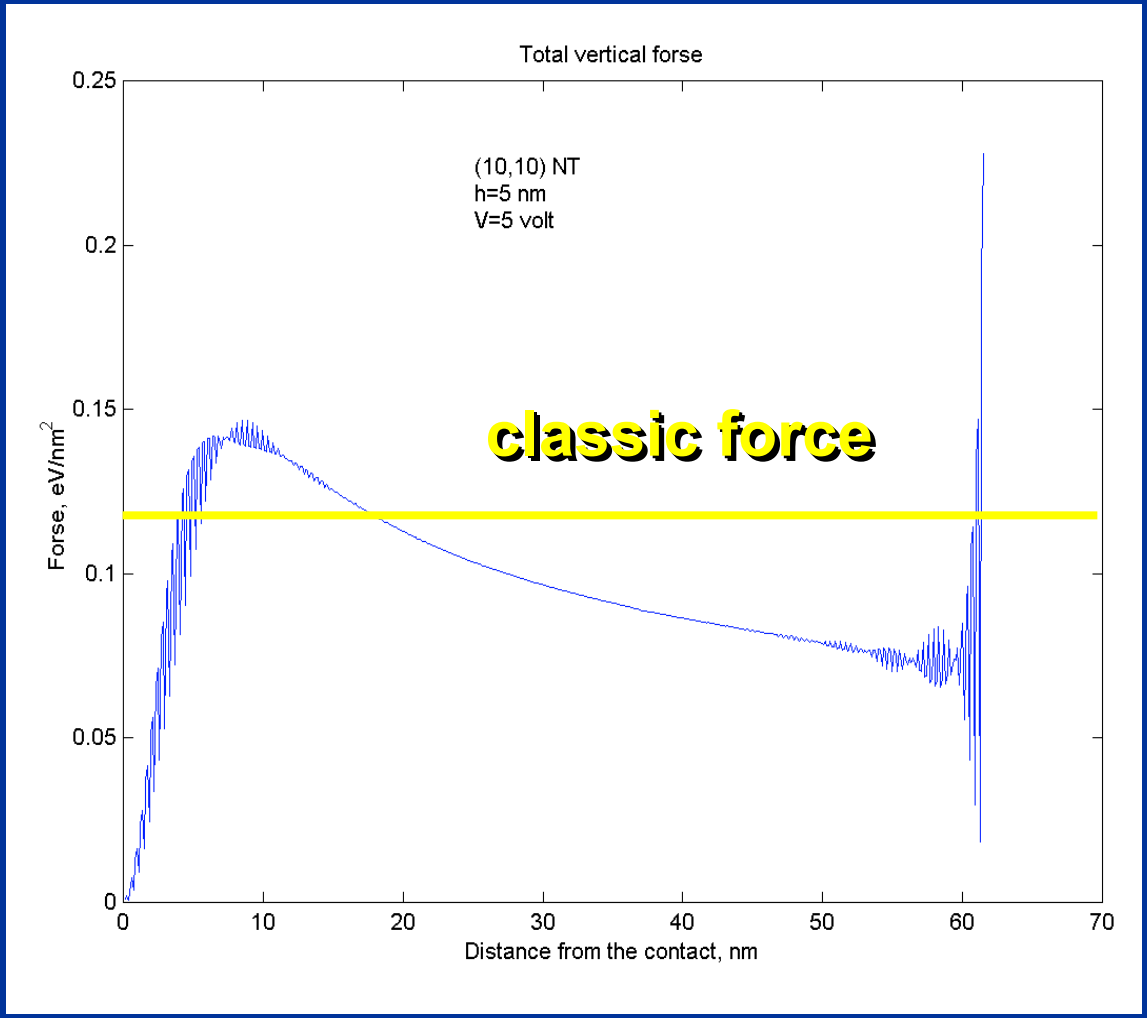

- Analytical Semiclassical (QM) calculation was compared with TBA and BP : correction is small because of high DOS

NT Transport Devices

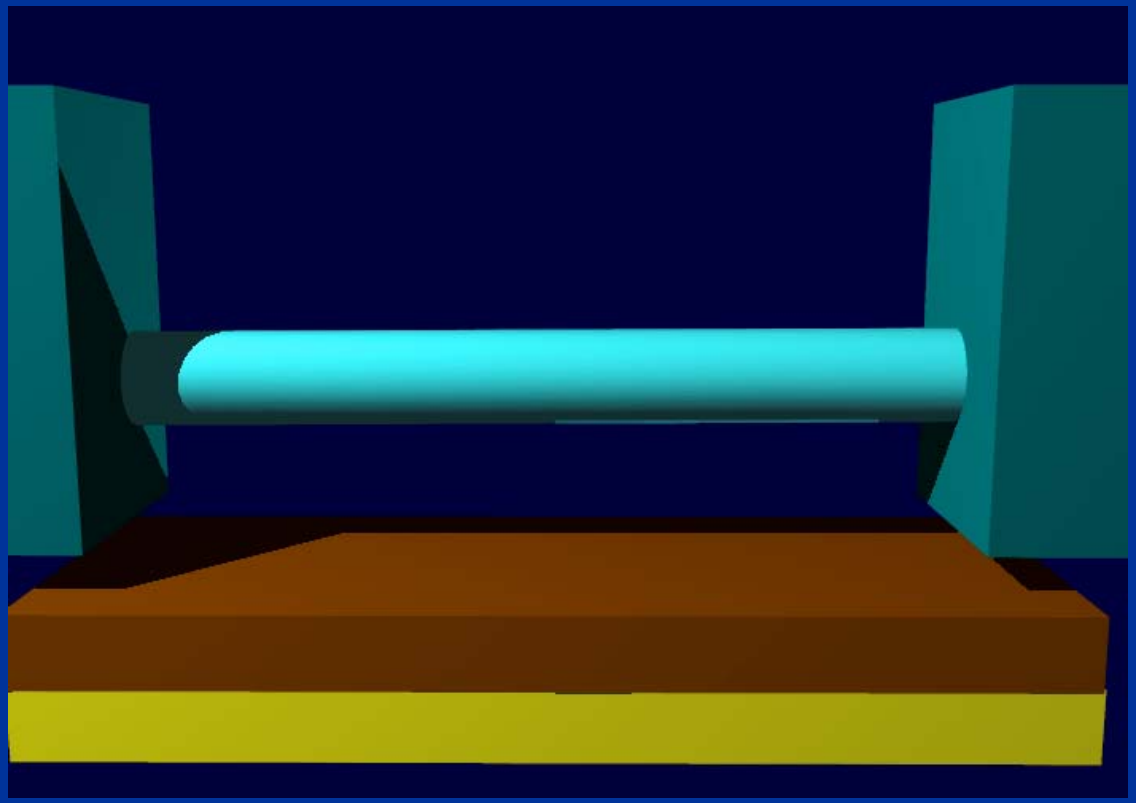

• The controlling transport in NT device by applying gate voltage opens possibilities for creating sensors, nanoelectronic devices, NEMS etc.

• Besides contact phenomena, the transport in NT devices differs from our experience for semiconductor devices:
  • different electrostatics (1D) results in a strong Coulomb interaction and, hence, in a strong depolarization
  • 1D transport may approach ballistic limit

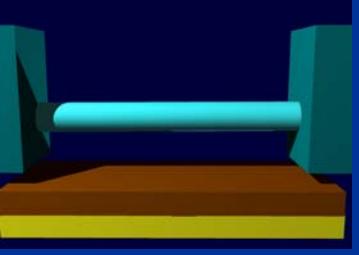

NT Transport Devices (2)

- Non-equilibrium charge is computed within drift-diffusion approximation

$$\frac{j}{e\mu} = n(x)\frac{d\phi^0}{dx} - C_t^{-1} n(x)\frac{dn}{dx}$$

$$n(x) = n_c + \Delta n_s(x)$$

$$\Delta n_0(x) = C_t \phi_c(x)$$

- We decompose the charge density into even and odd components
- and separate built-in charge

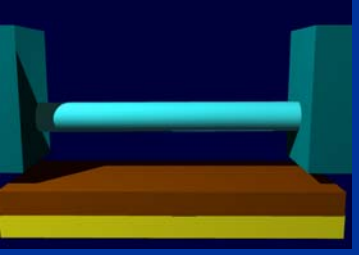

Equilibrium Charge Distribution

- Equilibrium charge distribution is calculated within the NT Compact Model for Electrostatics

- Comparison of different approximations for 40 nm long SWNT :
  - QM result in red
  - fully statistical approach in blue
  - Compact Model in dashed green

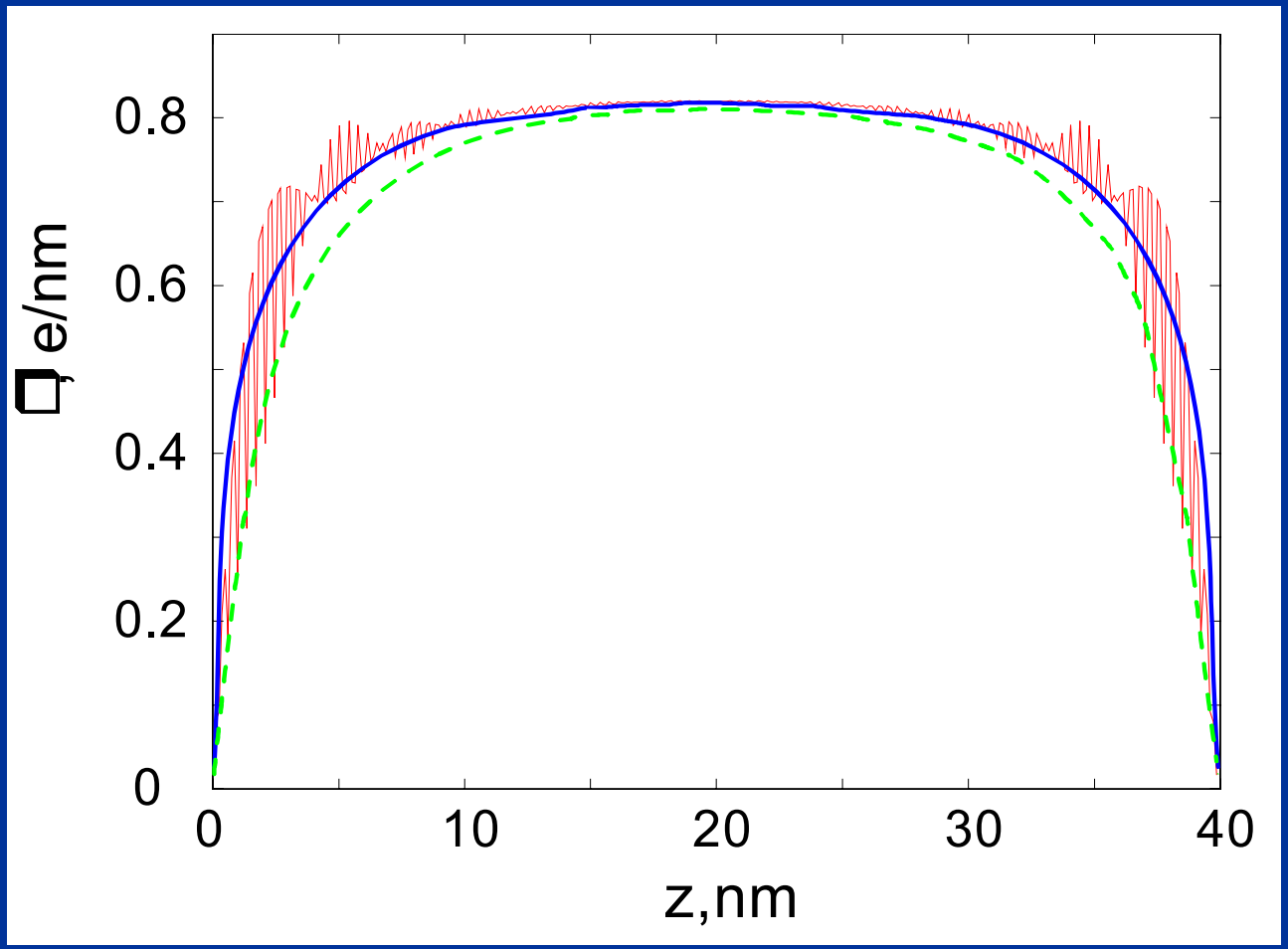

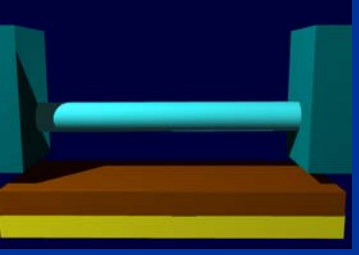

Linearization Approximation

- Linearization allows to obtain Ohm law for small V_d
  - equilibrium charge is proportional to the even part of the potential

$$\Delta n_s(x) = C_t\, \phi_s^0(x)$$

$$\phi_s^0(x) = \phi_c(x) + \phi_g(x)$$

- Solution for non-equilibrium charge density includes current

$$n_a(x) = C_t \left\{ \phi_a^0(x) + \frac{V_d}{2} - \frac{j}{e\mu} \int_{-L/2}^{x} \frac{dx'}{[n_c + \Delta n_s(x')]} \right\}$$

which is

$$j = \frac{V_d}{R}$$

where the resistance

$$R = \frac{2}{e\mu} \int_0^{L/2} \frac{dx}{[n_c + \Delta n_s(x)]}$$

Chemical Modification

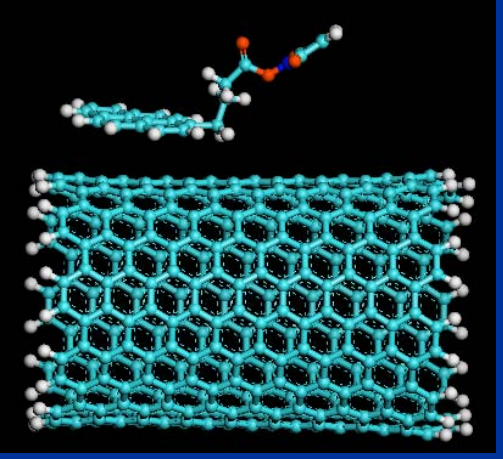

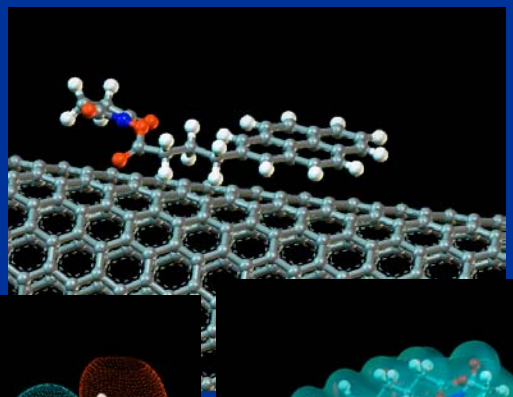

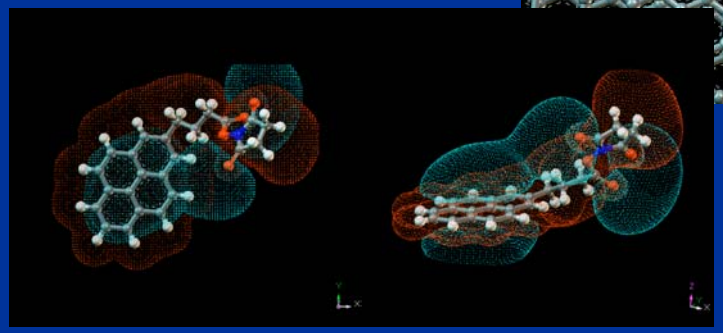

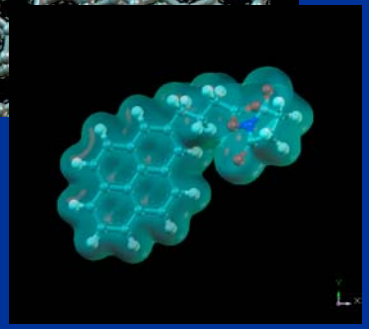

- Quantum-chemical study of organic molecule at SWNT surface showed
1) molecule structure/geometry has been changed
2) charge transfer may be essential as well as the complex polarization

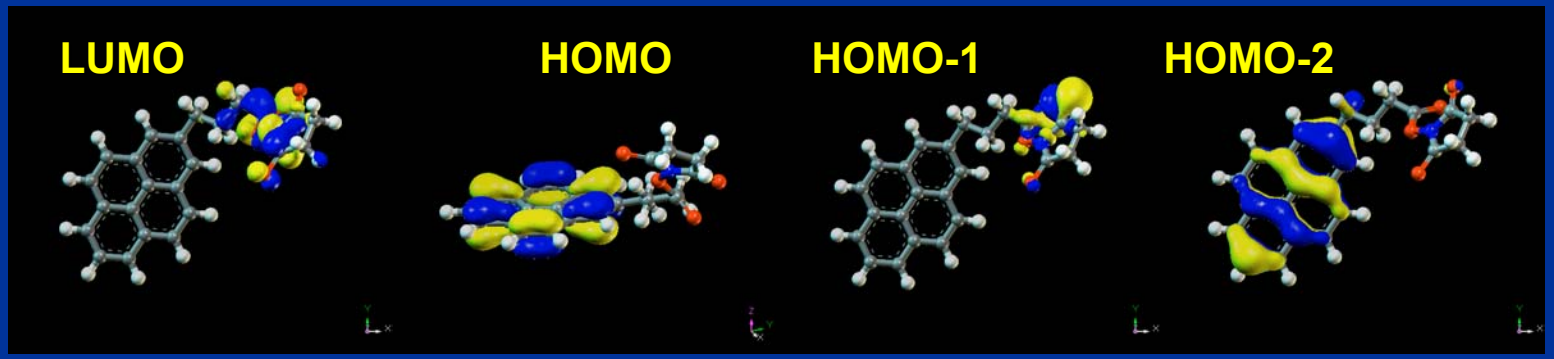

- Four levels near the Fermi energy have different symmetry and, hence, will create different potential on the SWNT

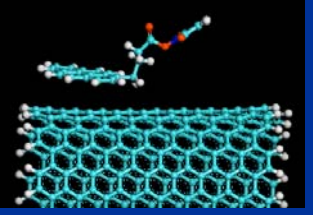

From Functionalization to Local Gate

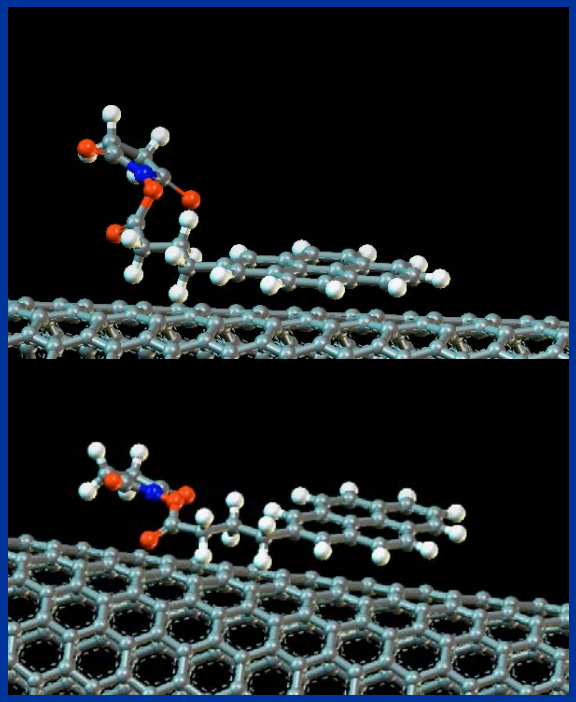

- As it is shown in subsequent MD snapshots, the complex flattens out

- We continue looking for a complex which attaches to SWNT and bring a charge in a controllable way

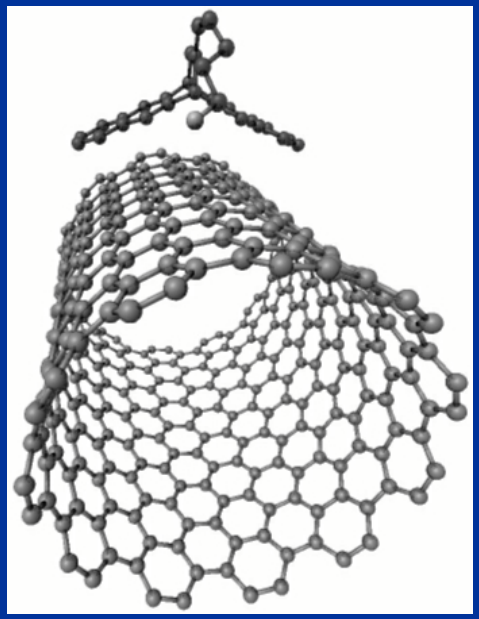

$$\frac{q}{\sqrt{(x - R\cos\alpha)^2 + (y - R\sin\alpha)^2 + z^2}}$$

- A “rider” molecule gently absorbs at the surface and can be ionized/polarized which locally changes SWNT conductance

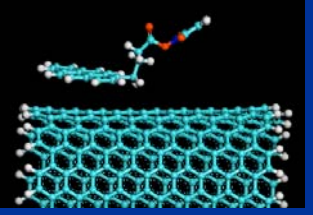

Local Gating of SWNT

$$\frac{C_Q^{-1}}{C_g^{-1}}\left(\frac{q}{\sqrt{R^2+\rho^2+z^2}}-\frac{q^*}{\sqrt{R^2+\rho^2+4h\rho\sin\varphi+4h\rho^2+z^2}}\right)$$

selfconsistent potential with image charge

$$q^* = -q\frac{\varepsilon-1}{\varepsilon+1}$$

depolarization by the SWNT is given by the Compact Model

$$\phi^{act} = \frac{C_Q^{-1}}{C_g^{-1}+C_Q^{-1}}\phi^{xt} \simeq \phi^{xt}\,\frac{C_Q^{-1}}{C_g^{-1}}$$

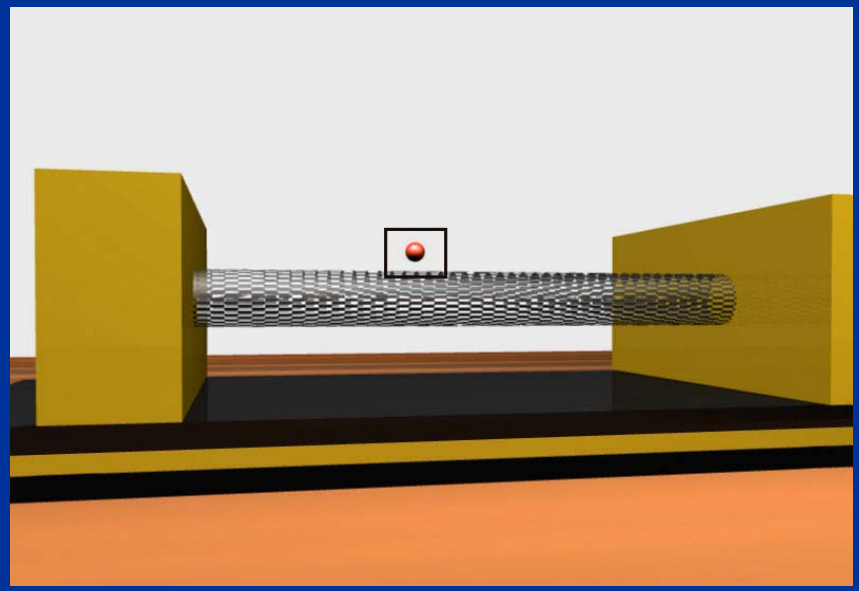

- **Local gating is due to electric potential developed in proximity to the charged complex - “rider”-molecule**

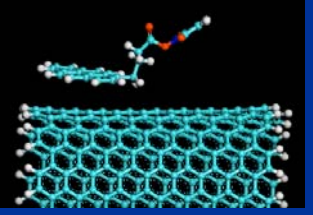

Local Gating of SWNT

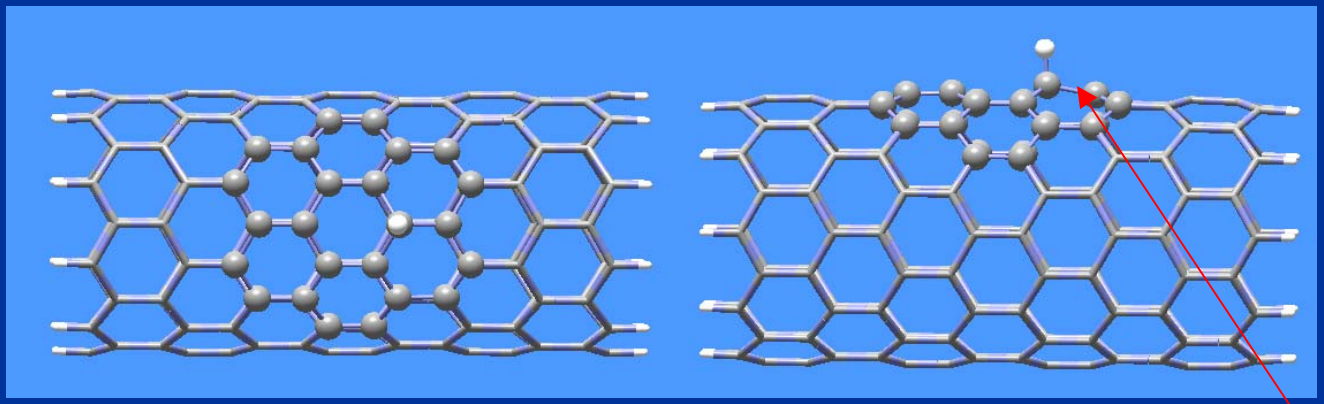

H^+ - +0.4e

NH_4^+ - +0.9e

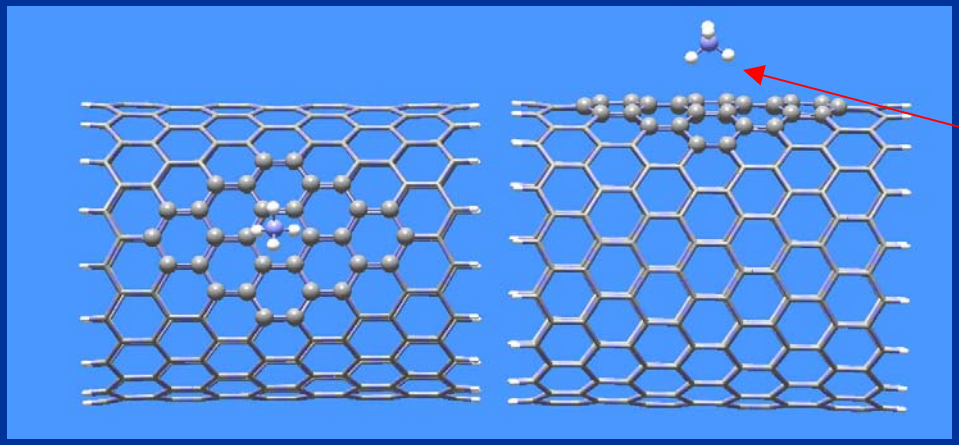

DFT/UFF within ONIOM in Gaussian-98

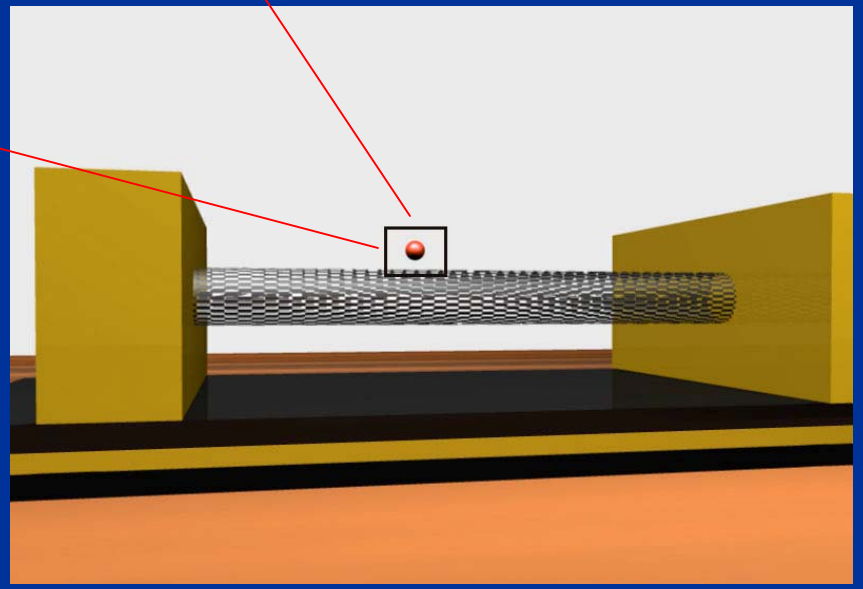

- Two simple examples of charged rider-molecules (candidates for LCG): a single proton and an ammonium ion

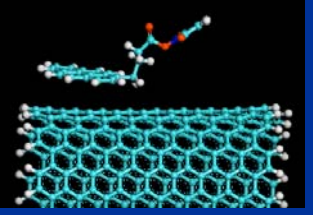

Local Gating of SWNT (2)

- Coulomb potential of a remote impurity depends on the angular position of the charge because of the substrate screening

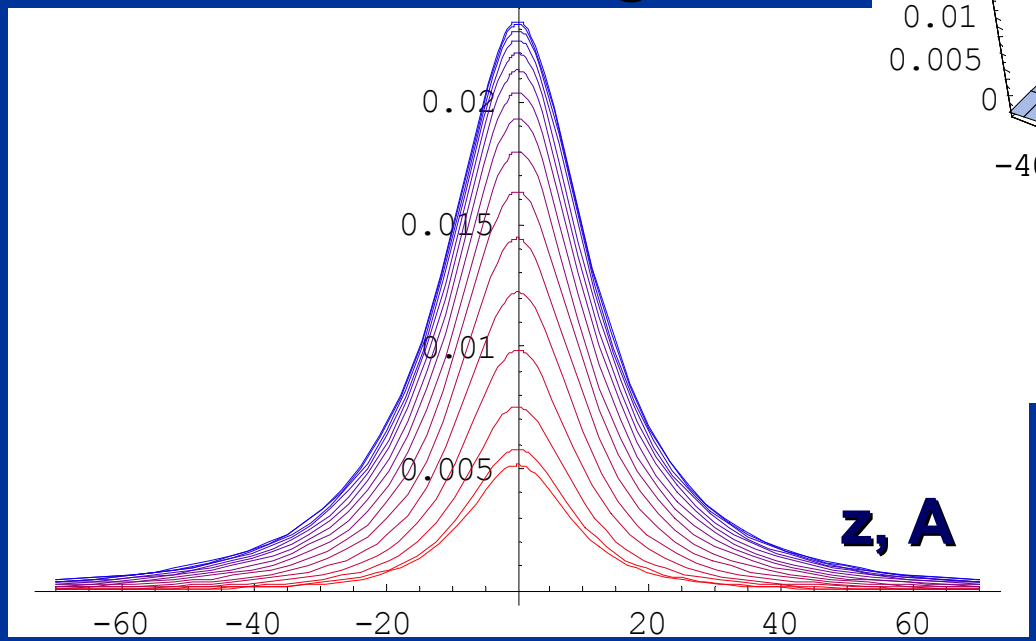

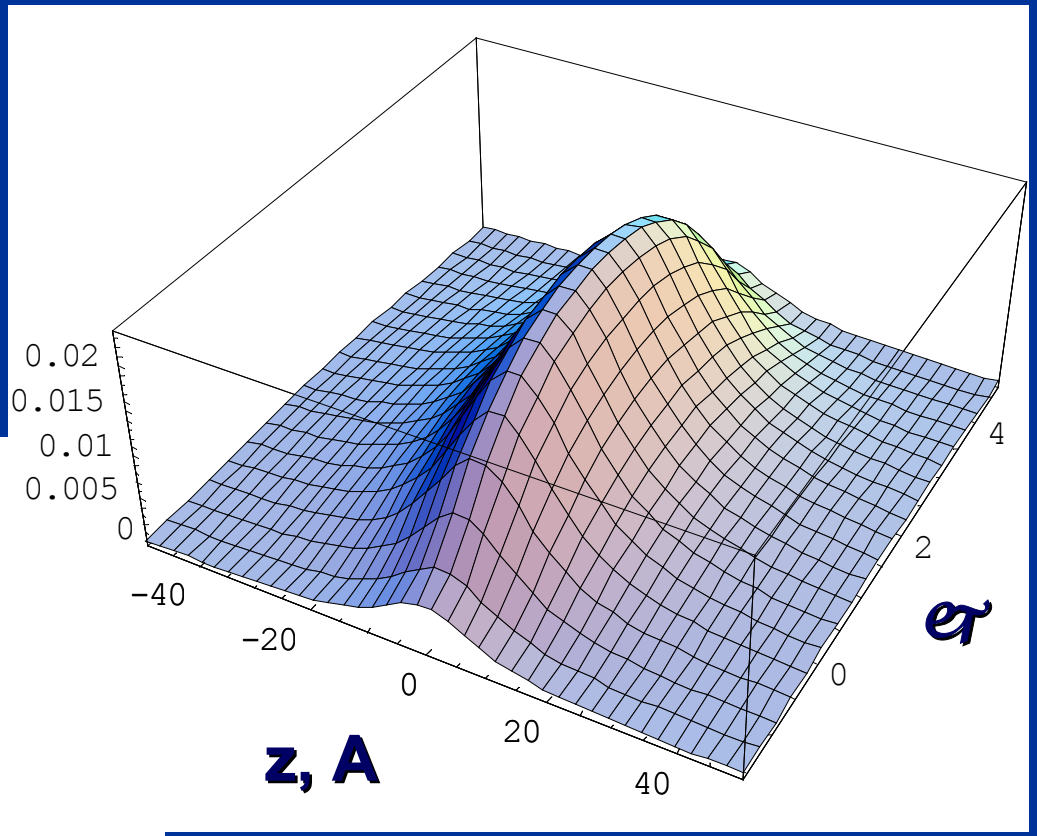

$$2q(\varepsilon/2+1/2)h(\rho+h)C_Q^{-1}/z^3C_g^{-1}$$

- Characteristic length scale of the screened Coulomb potential along the SWNT is several nm, potential decays as z^3

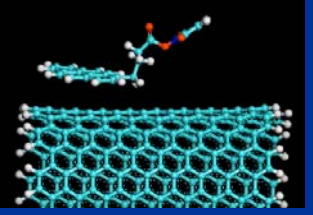

Local Gating of SWNT (3)

$$\mathcal{T}(E) = \frac{1}{1 + \exp[-2\pi \frac{E - U_o}{\hbar} \sqrt{\frac{m^*}{\partial^2 U / \partial z^2}}]}$$

Transmission coefficient as a function of energy of incoming electron for different rider angles on the NT surface

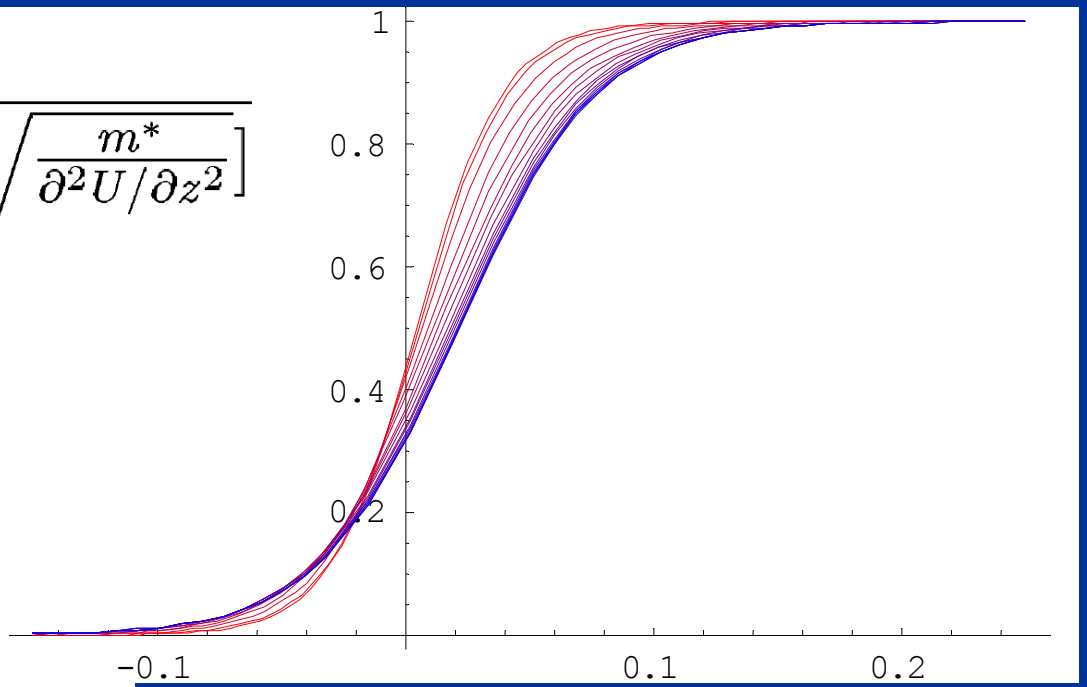

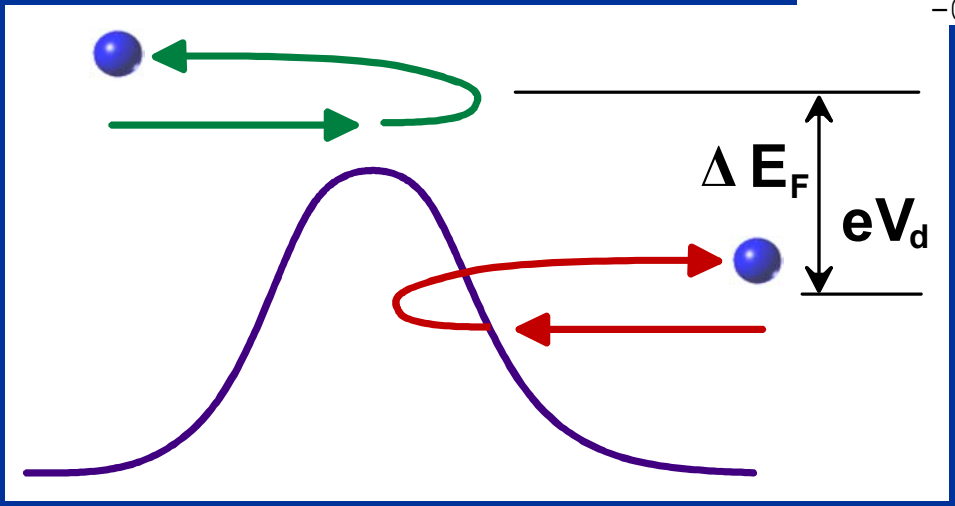

- **Ballistic current depends only on the difference of the chemical potentials at the right and left sides of the device and transmission probability at Fermi level**

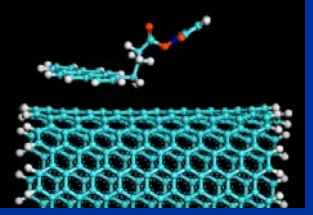

Local Gating of SWNT (4)

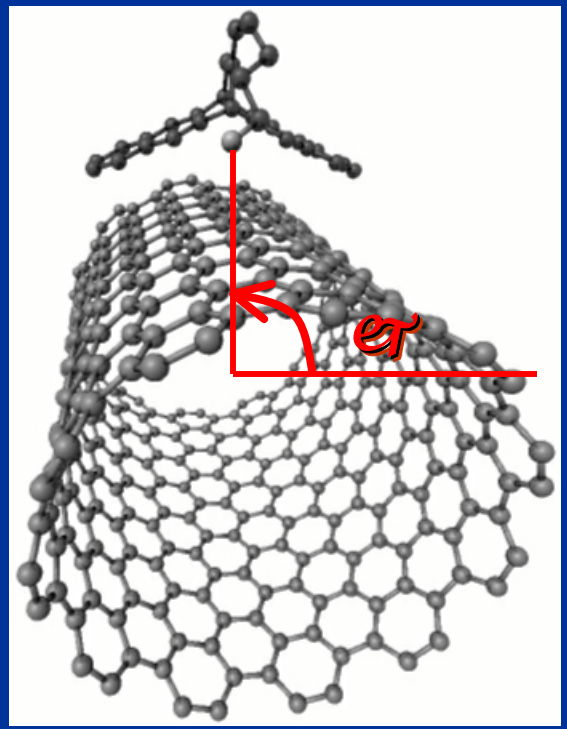

$$G_o = e^2/h$$

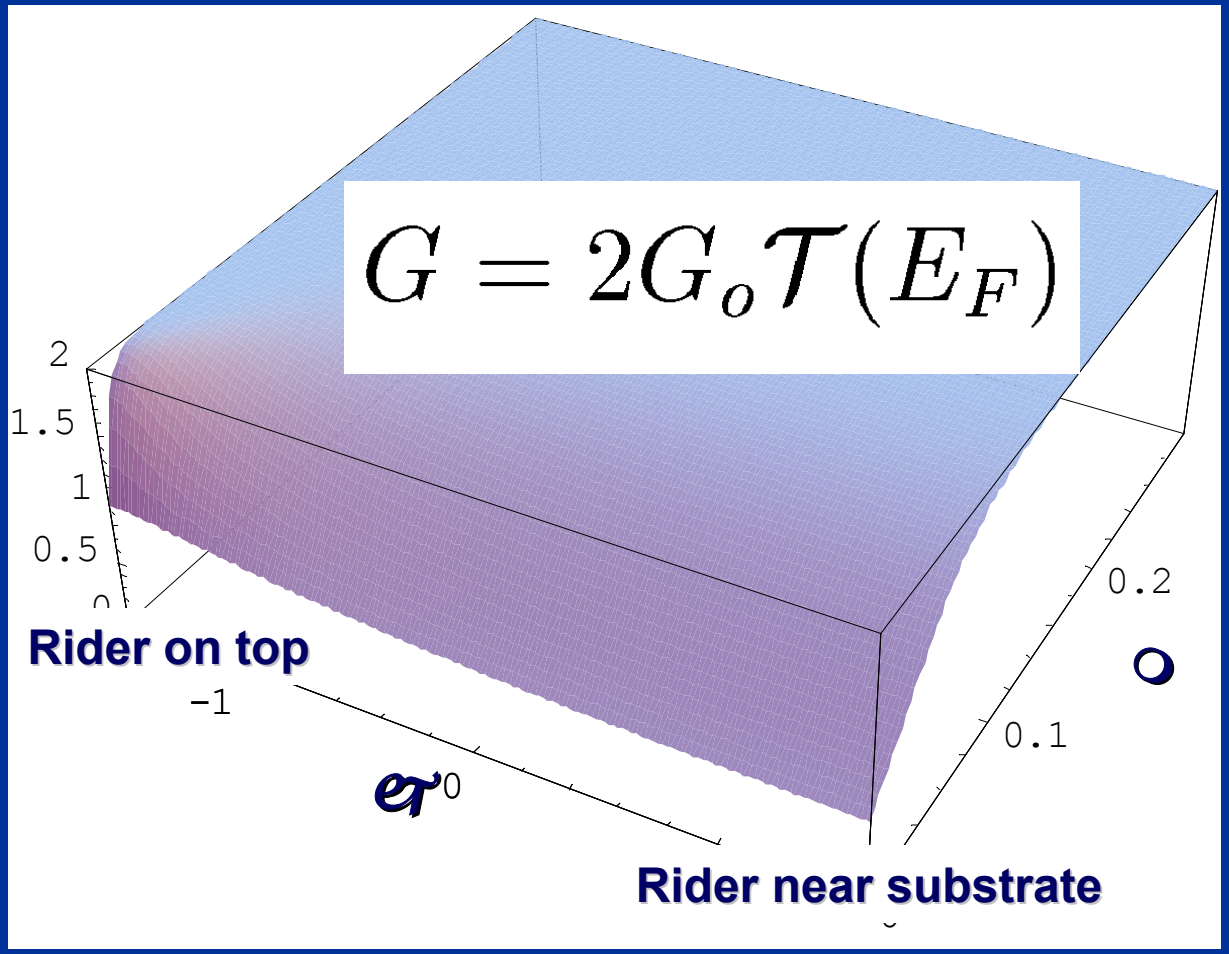

- Conductance as a function of the chemical potential and the angular position of the rider on the nanotube surface

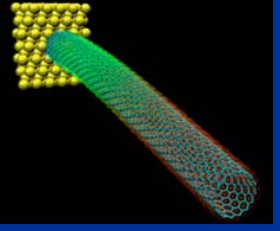

Why move beyond standard MEMS theory

- NEMS (nanotube electromechanical system) operation involves new physics: vdW forces, *e.g.*

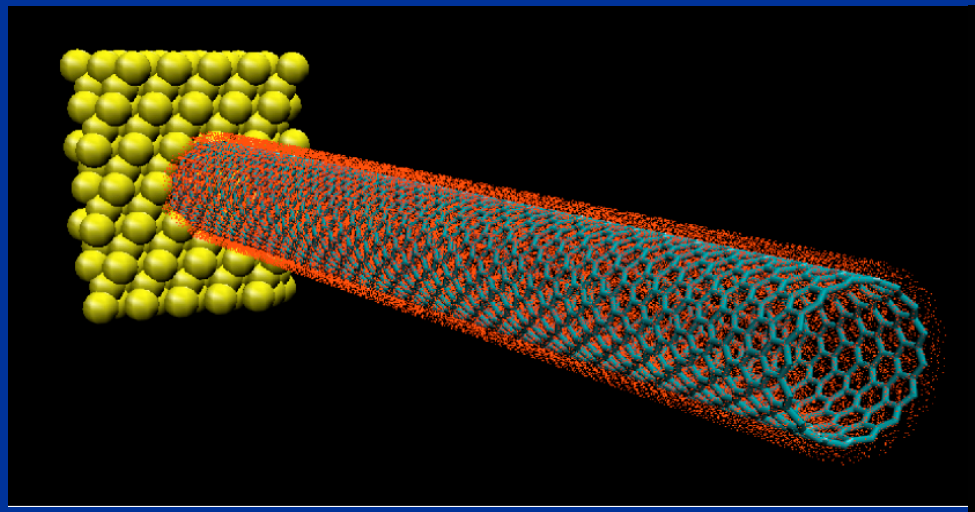

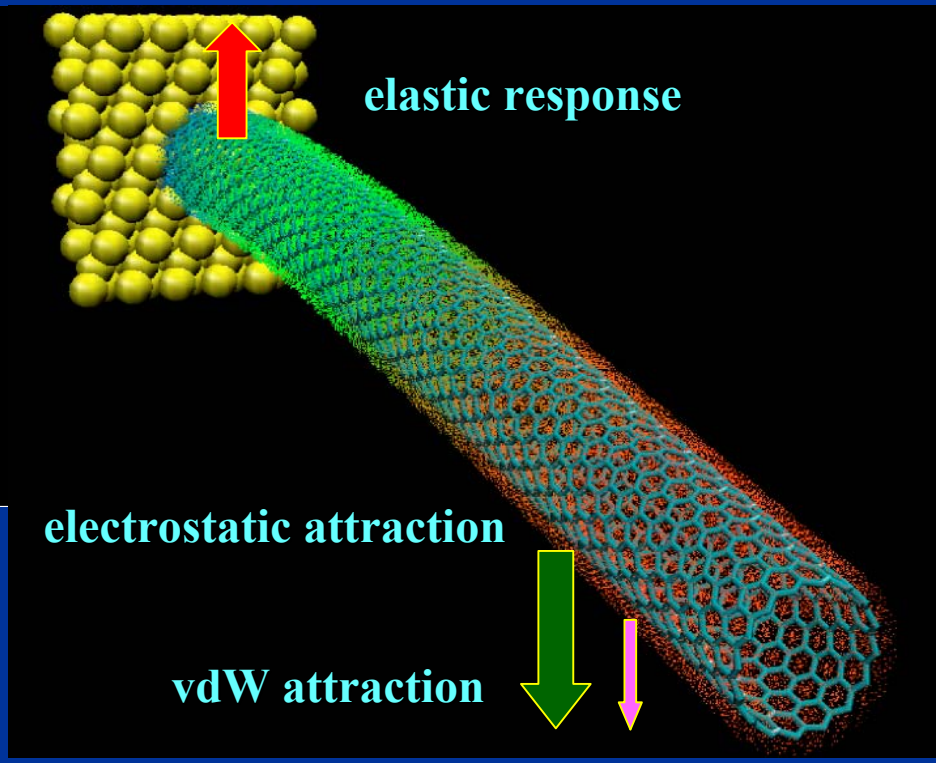

- OFF and ON states of a simplest actuator are controlled by three forces: elastic, electrical and vdW

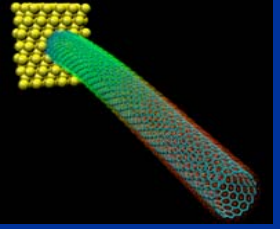

MD parametrization of Continuum Elasticity

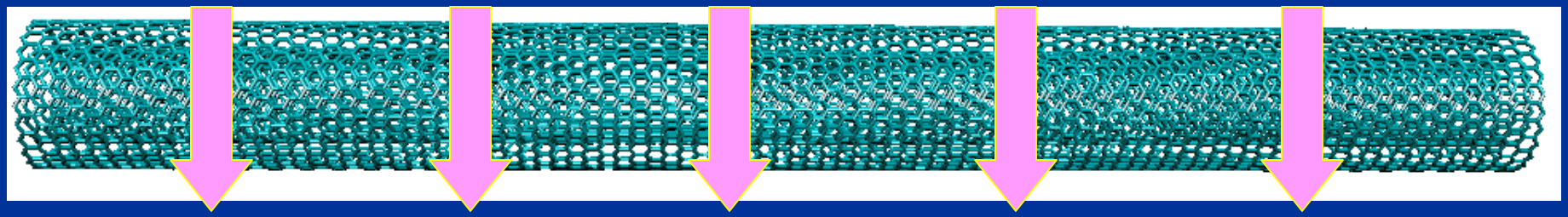

- Geometry of simulation: fixed-fixed DWNT L=20nm, R=1nm

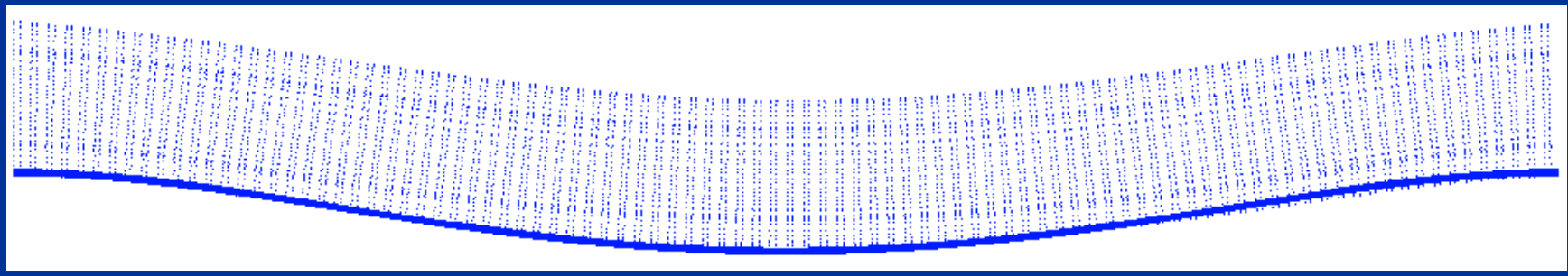

- Beam theory gives the same shape as MD at E~1.2 TPa

Marc Dequesnes, Slava V. Rotkin, Narayan R. Aluru, Int.J.Comp.Electronics (2002).

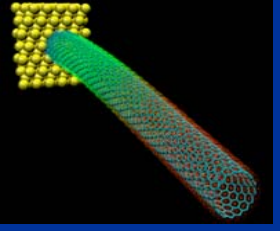

Simulation of Nanotweezers

- **System becomes unstable at certain voltage which is the pull-in voltage**

Experimental results: S. Akita *et. al* (2001)

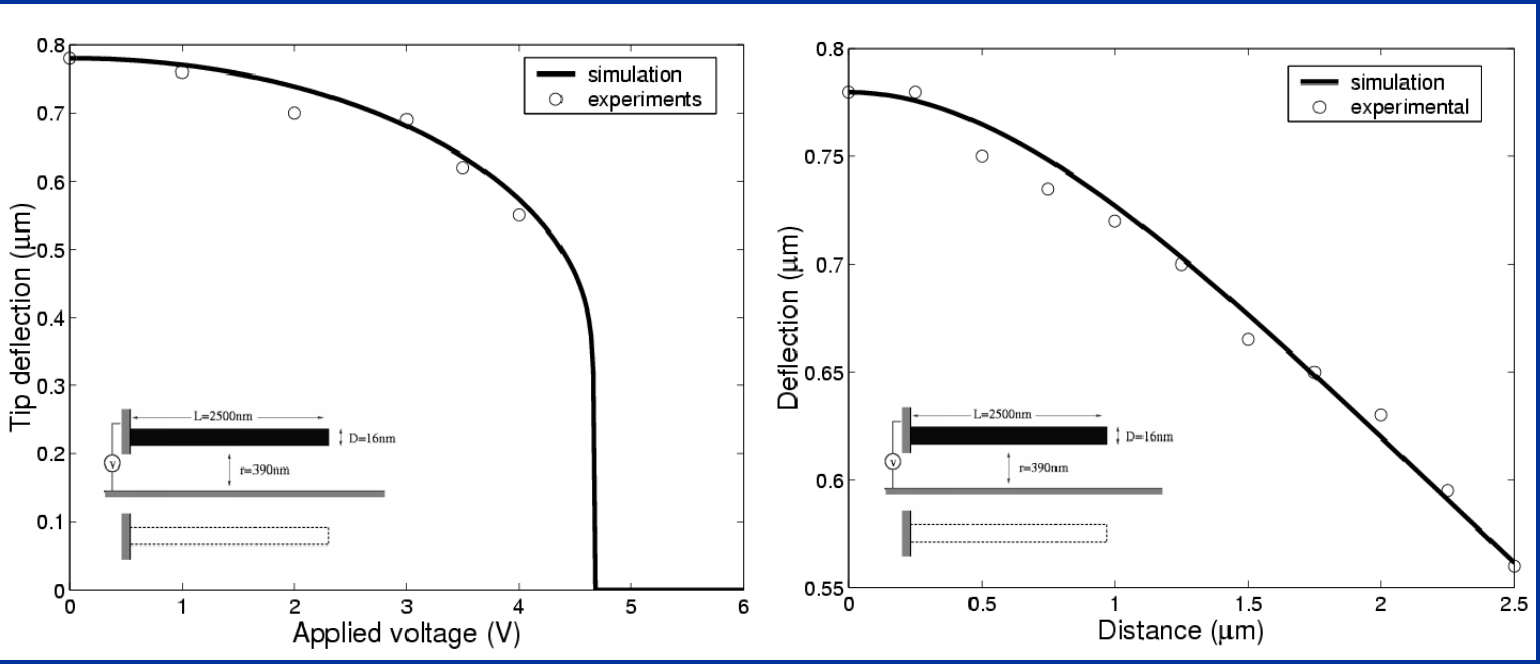

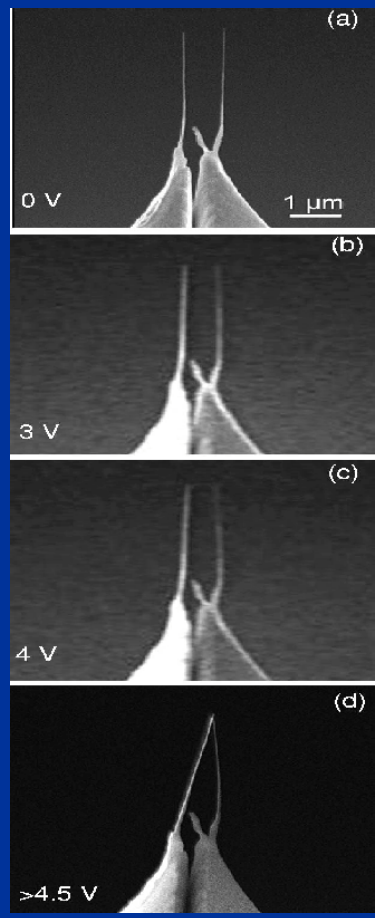

Theory: Marc Dequesnes, Slava V. Rotkin, Narayan R. Aluru, Calculation of pull-in voltages for carbon nanotube-based nanoelectromechanical switches, Nanotechnology **13**, 120-131, 2002

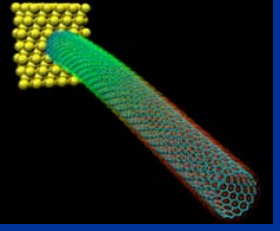

NEM Switches: Role of vdWE in the Optimum Design

- **Van der Waals forces manifest itself in pull-in of cantilever device because of lower stiffness. The pull-in gap decreases.**

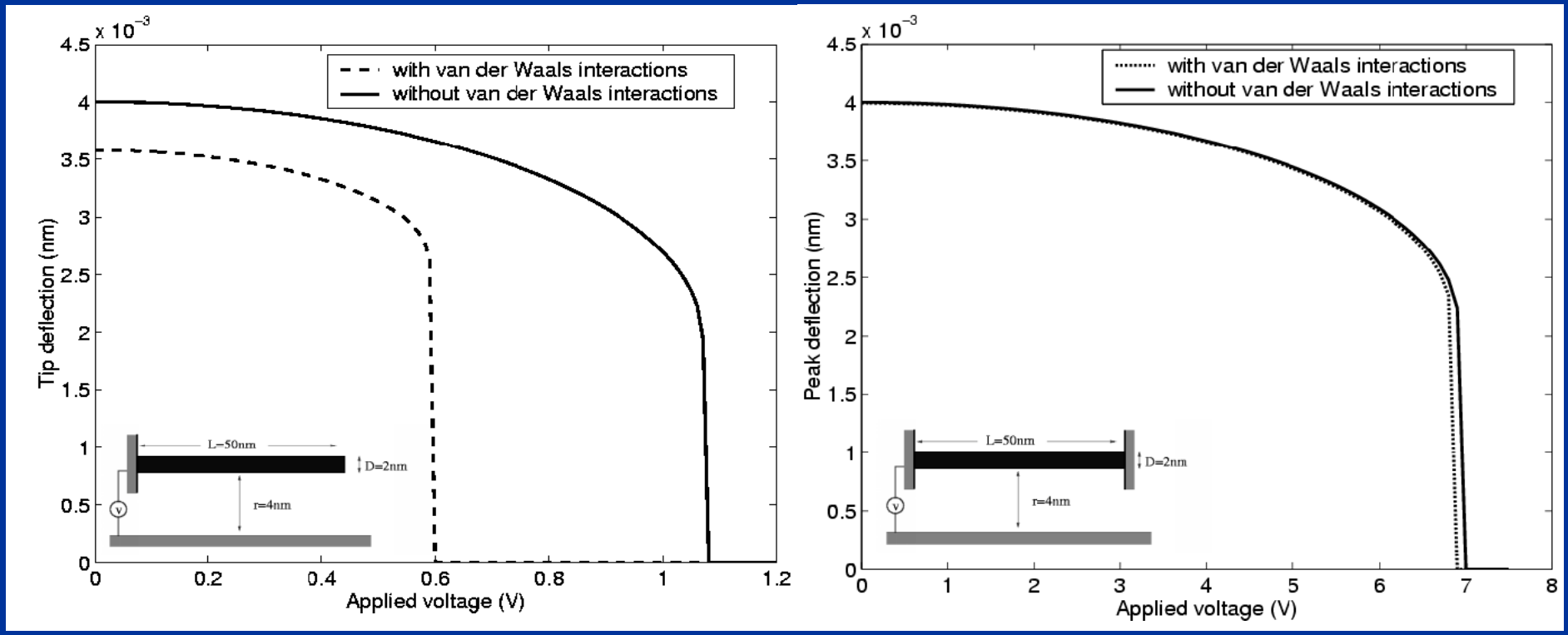

DWNT : L=50 nm, R=1 nm, h=4 nm

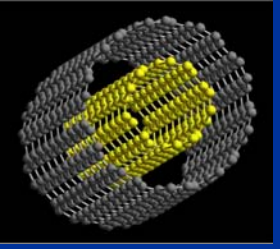

Analytical Theory for the Pull-In at the Nanoscale

- In order to be able to predict behavior of various NEMS an analytical theory has been developed
- It works with the minimization of a total energy comprised of three terms in a simplest case

$$E(x,\varphi) = T(x,h;k) - V(x,\varphi;C) - W(x;\epsilon,\alpha)$$

$$V = C\varphi^2/2$$

- electrostatic energy

$$T = k(h-x)^2/2$$

- elasticity

- Van der Waals forces

$$W \simeq \epsilon x^{-\alpha}$$

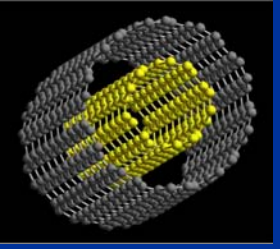

Analytical (2): Stability

- The pull-in phenomenon is an instability of the solution for device equation. In terms of total energy the conditions are:

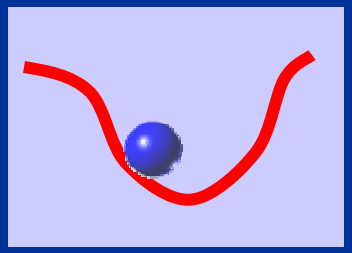

system equilibrium

$$\frac{\partial E}{\partial x} = 0$$

$$\frac{\partial^2 E}{\partial x^2} = k - \frac{\varphi^2}{2}\frac{\partial^2 C}{\partial x^2} - \frac{\partial^2 W(x)}{\partial x^2} = 0$$

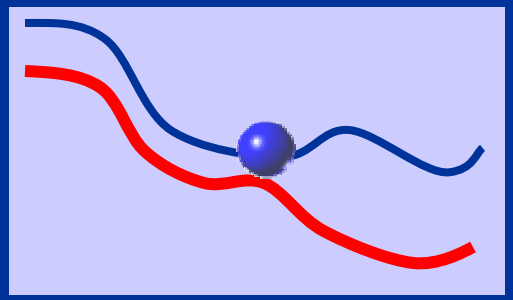

instability point

- If vdW force and capacitance depend on normal coordinate in a standard way simple functions

$$W \simeq \epsilon x^{-\alpha} \qquad C = c_o/x$$

derivatives are

$$\partial C/\partial x = -C/x \qquad \partial^2 C/\partial x^2 = 2C/x^2$$

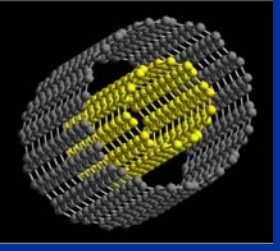

Analytical (3): Example of Planar MEMS

- First, neglecting van der Waals force the pull-in x_o and V_o:

$$x_o|_{W\to 0} = \frac{\beta_2}{\beta_1+\beta_2} h \,|_{\beta\to 1} = \frac{2}{3} h$$

$$\beta_1 = 1,\ \beta_2 = 2$$

planar MEMS

$$V_o|_{W\to 0} = \frac{\sqrt{\beta_2}}{\beta_1+\beta_2} \frac{\sqrt{2kh}}{\sqrt{C(x_o)}} |_{\beta\to 1} = \frac{2}{3} \frac{\sqrt{kh}}{\sqrt{C(x_o)}}$$

are given as functions of logarithmic derivatives of the electrostatic potential.

As a consistency check, the MEMS result is easily reproduced

$$V_o(0) \propto h^{3/2}$$

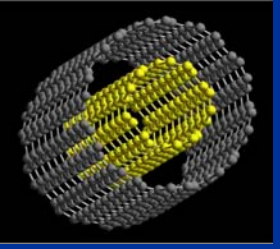

Analytical (4): vdW terms

- Including van der Waals potential

$$\begin{cases} x_o = \dfrac{2}{3}h\left(\dfrac{1}{2}+\dfrac{1}{2}\sqrt{1+3\alpha(\alpha-1)\dfrac{W(x_o)}{kh^2}}\right) \\ V_o = \dfrac{2\sqrt{k}h}{3\sqrt{C(x_o)}}\sqrt{\dfrac{1}{2}-\dfrac{3}{2}\alpha(\alpha+2)\dfrac{W(x_o)}{kh^2}+\dfrac{1}{2}\sqrt{1+3\alpha(\alpha-1)\dfrac{W(x_o)}{kh^2}}} \end{cases}$$

- Explicit expressions for the pull-in voltage and gap show that vdW energy at the pull-in gap has to be comparable with the elastic energy at the initial separation to be able to observe new effects: this is the case for nanoscale NEMS

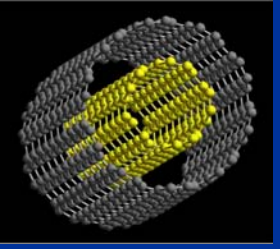

Analytical (5)

- For practical application, one has to keep only linear terms in the expression

$$\begin{cases} x_o \simeq h\dfrac{2}{3}\left(1+\dfrac{3}{4}\alpha(\alpha-1)\dfrac{W(x_o)}{kh^2}+o(W/kh^2)\right) \\ V_o \simeq \dfrac{\sqrt{k}}{\sqrt{c_o}}\left(\dfrac{2}{3}h\right)^{3/2}\left(1-\dfrac{9}{4}\alpha\dfrac{W(x_o)}{kh^2}+o(W/kh^2)\right) \end{cases}$$

The results of the analytical theory are

- the vdW decreases the operation range of the NEMS (by increasing the pull-in gap)
- when scaling down the device size, a principal limit of operation will be reached, which is due to V_o goes to zero

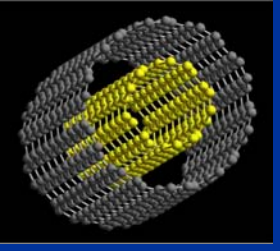

NEM switches: vdWE sets a Principal Physical Limit

- Van der Waals forces lower an operation range of NEMS
- Scaling down of the NEMS is limited by vdW critical size

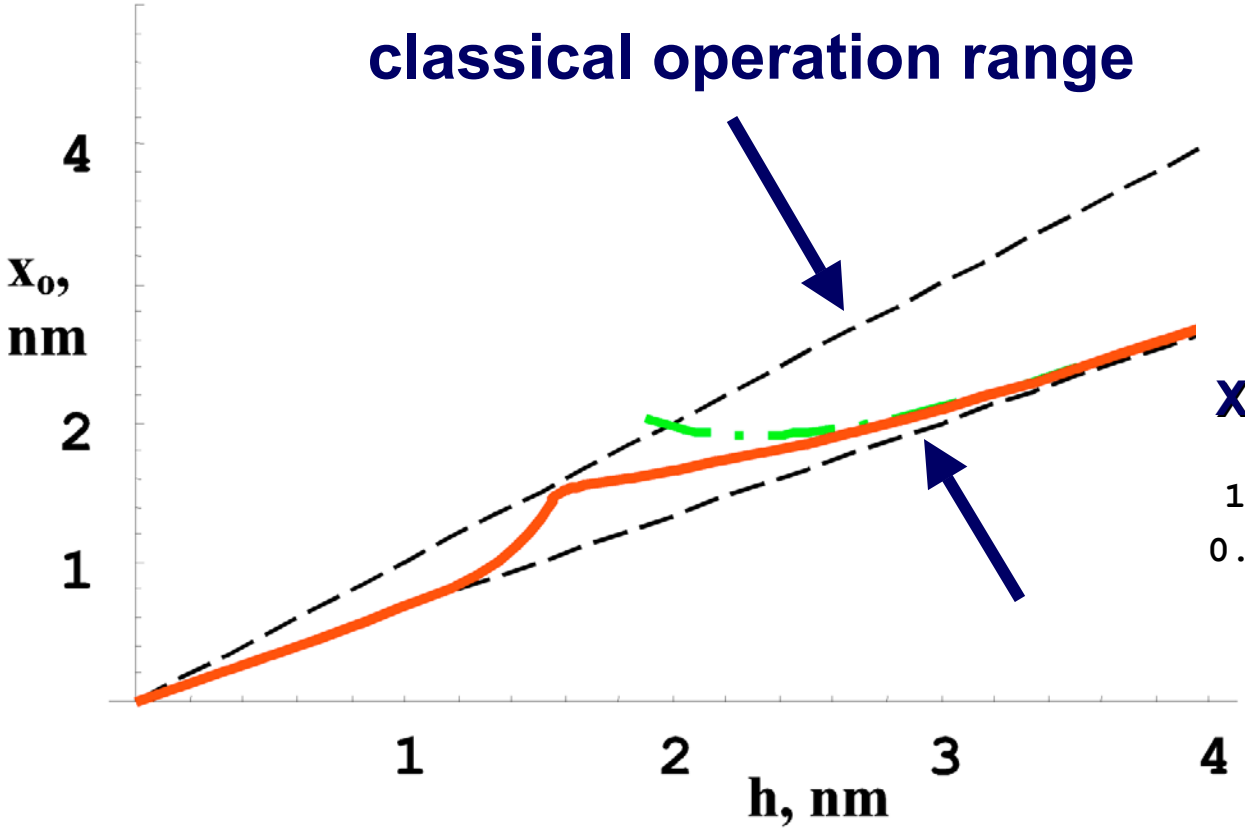

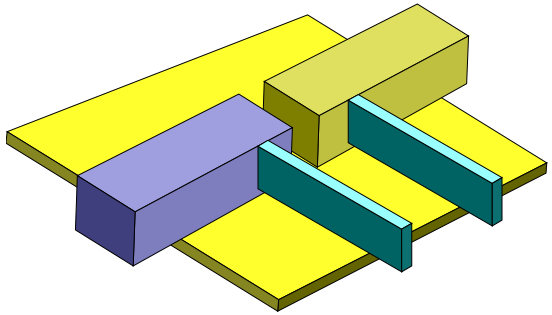

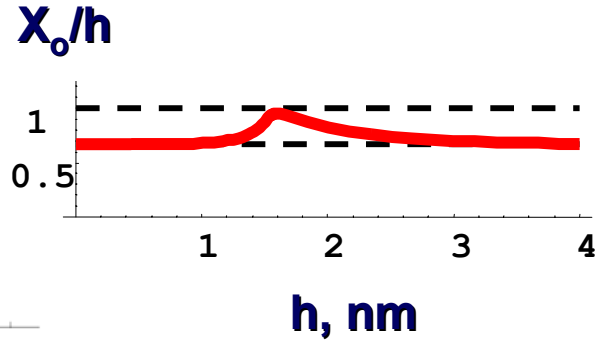

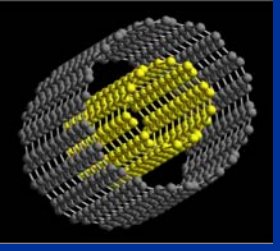

NEM switches: vdWE sets a Principal Physical Limit (2)

- The pull-in voltage does not scale down as a 3/2 power law as predicted by classical MEMS theory. Instead, it drops at h_c

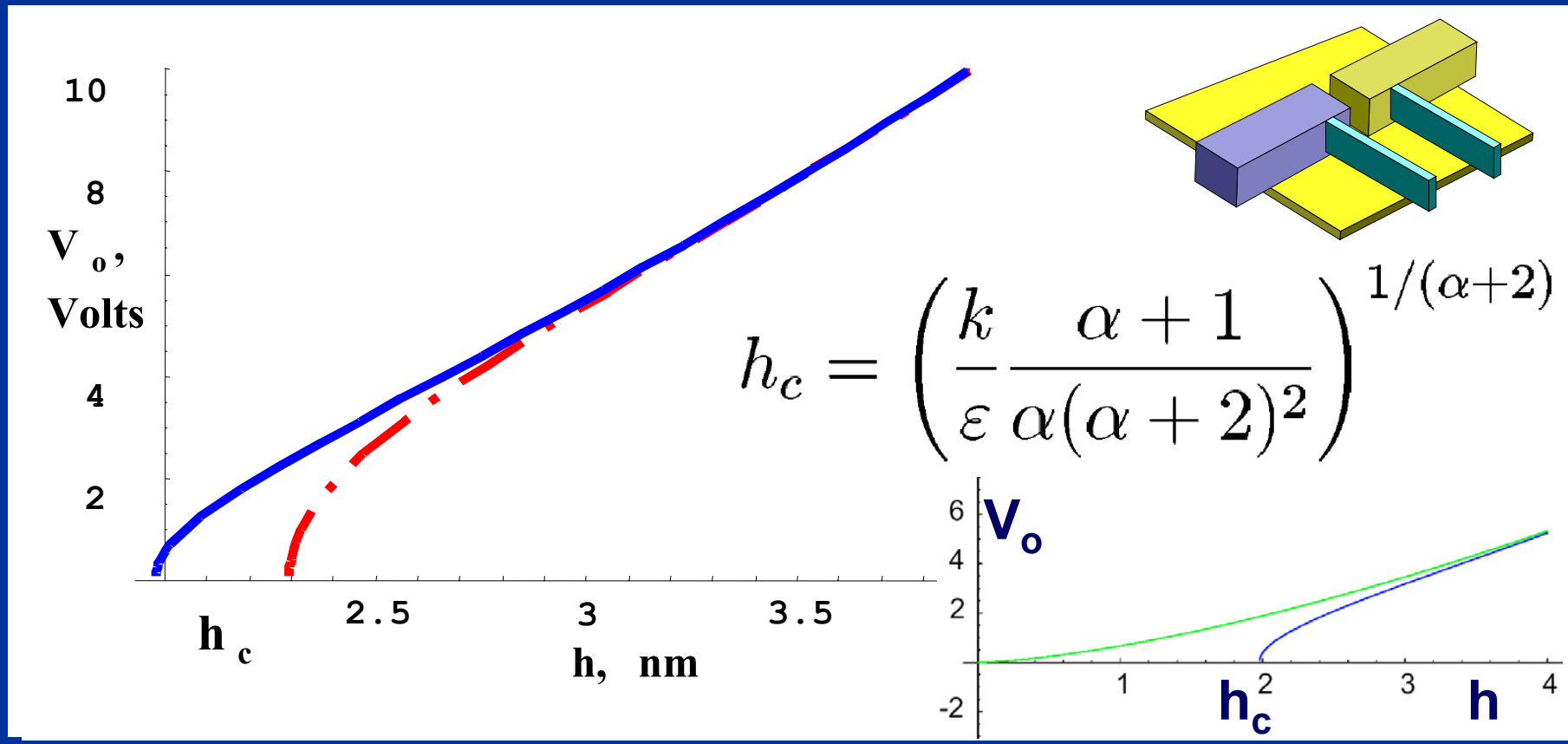

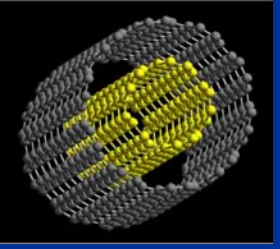

Nanotube NEMS

- Nanotube based NEMS devices have different electrostatics
- It is favorable in terms of the device operation range
- though, the operation voltage is high

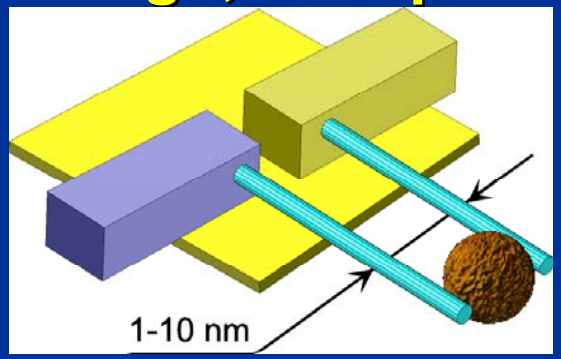

$$\beta_1 = C$$

$$\beta_2 = C(2C+1)$$

$$\begin{cases} x_o = h\dfrac{\frac{1}{2}C^{-1}+1}{C^{-1}+1} \\ V_o = \dfrac{\sqrt{k}h\sqrt{\frac{1}{2}C^{-1}+1}}{\sqrt{C}(1+C)} \end{cases}$$

$$\begin{cases} x_o \simeq h\dfrac{1}{2}\left[1+C\left(\dfrac{h}{R}\right)+o(C)\right] \\ V_o \simeq \dfrac{\sqrt{k}hC^{-3/2}\sqrt{\frac{1}{2}C^{-1}+1}}{(C^{-1}+1)}\left[1+o(C)\right] \end{cases}$$

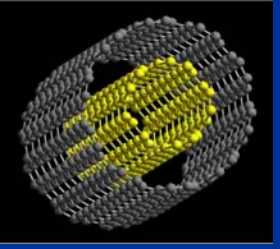

Quantum Capacitance of a NT device for NEMS

- The analytical expressions for the pull-in voltage and gap of a NT device are different from a MEMS result: the device operation range is larger for NT devices

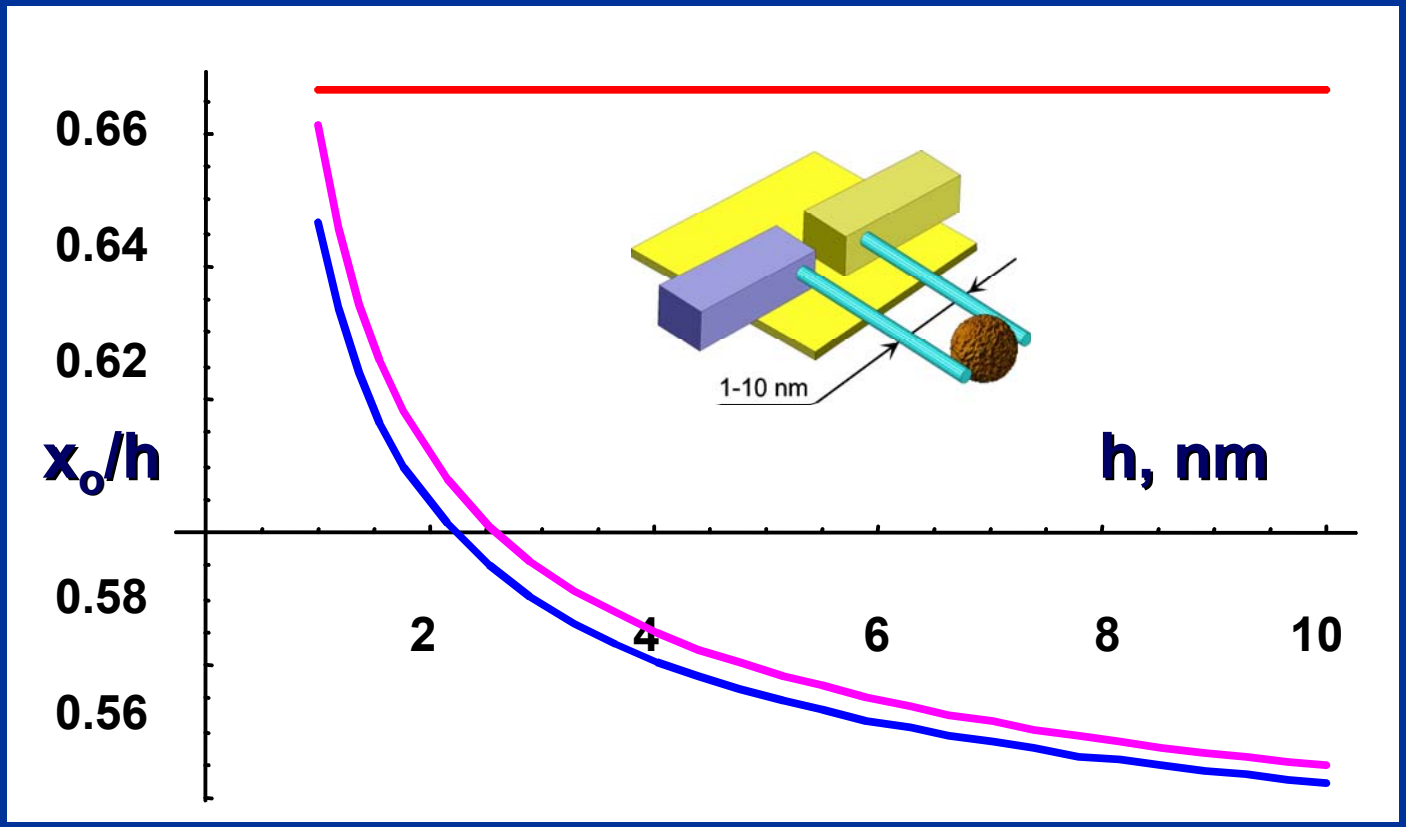

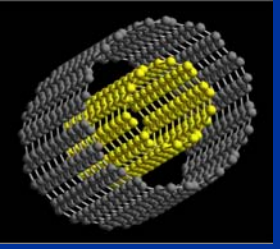

Quantum Capacitance of a NT device for NEMS (2)

- The pull-in voltage is much larger than a classical MEMS result (effect does not disappear for large Om scale)

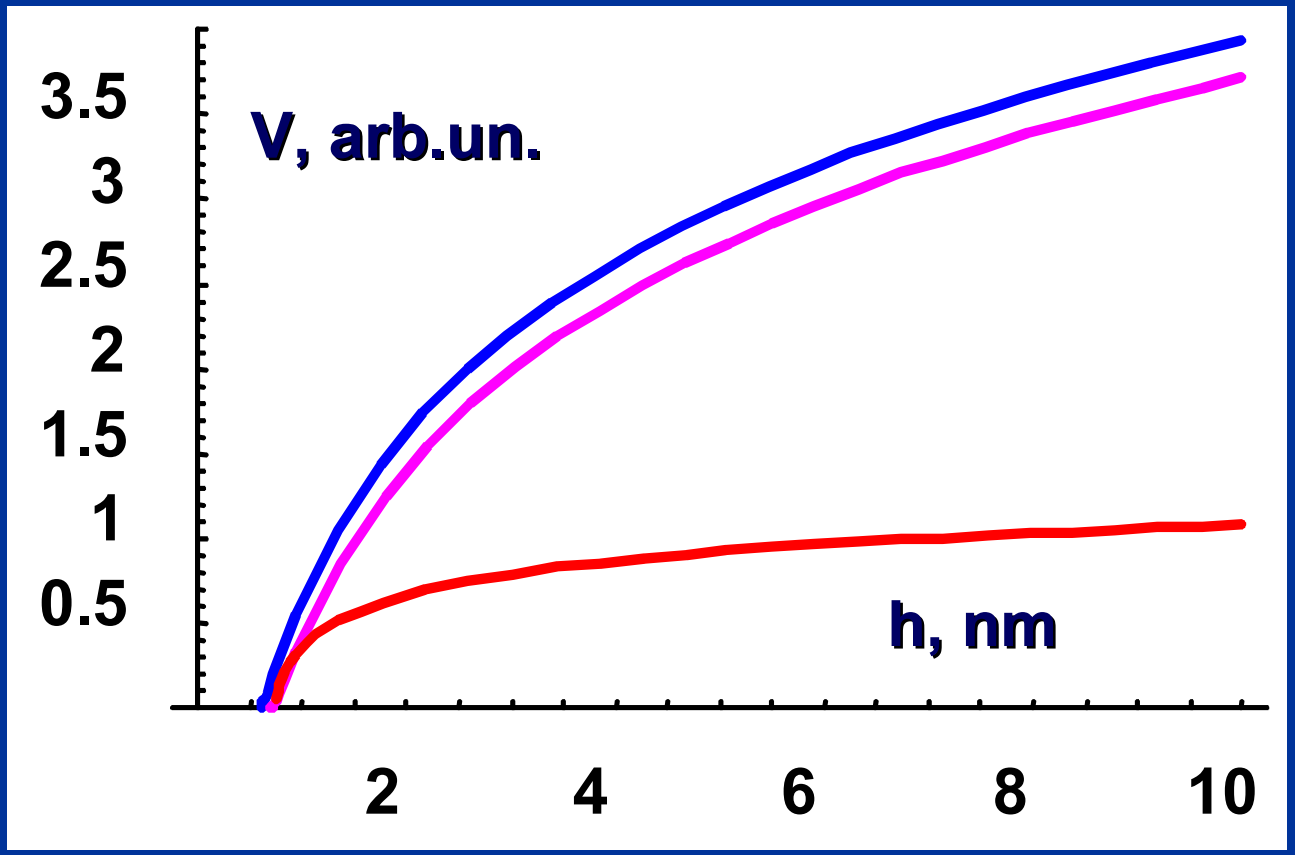

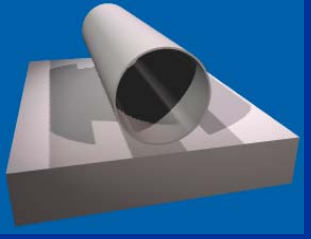

Quantum Correction for vdWf

- Calculation of the van der Waals interaction in NEMS and other systems (e.g. biological and artificial Ion Channels)
- Three systems have been computed DWNT, SWNT-on-Me, 2-SWNTs

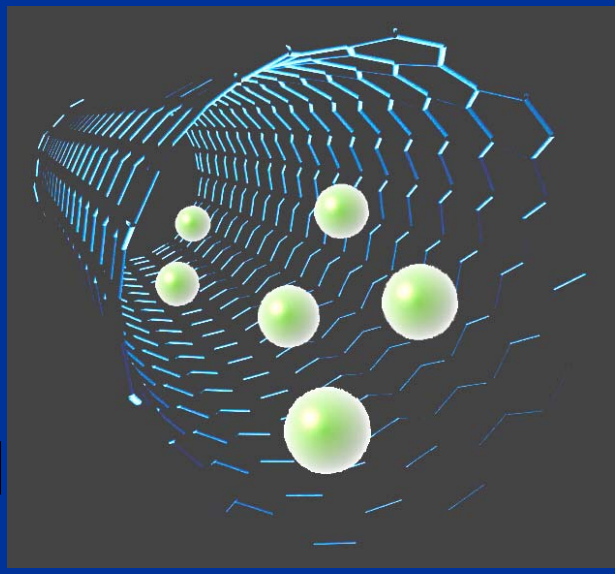

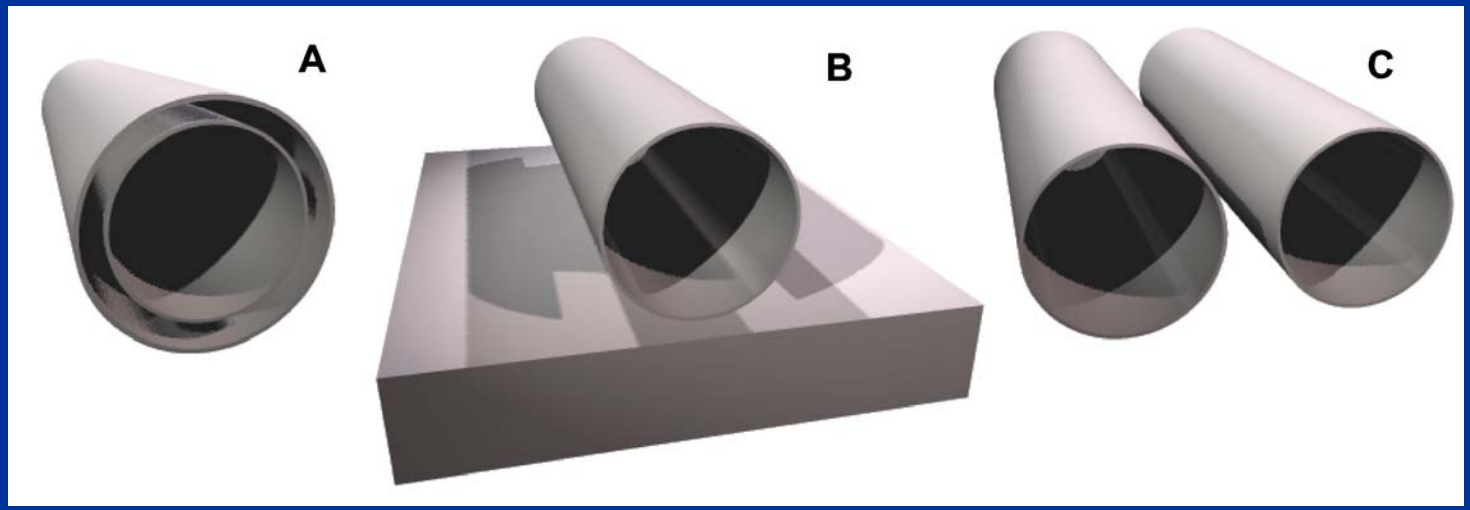

Slava V. Rotkin, Karl Hess, Int. Journal of Comp. Electr. (2002).

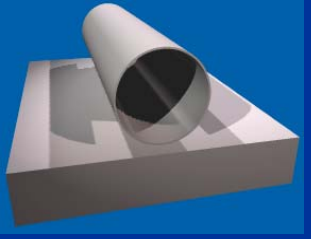

When vdW Quantum Correction term is important

- For Si (and other non-carbon) substrate the vdW interaction may have only delocalised mode term
- For pure carbon system (NT on HOPG, MWNT etc) with incommensurate lattices (at certain NT orientation) the sum of individual atom vdW forces can decrease almost to zero (A.Zettl, R.Ruoff, K.Miura)
- For Biological Ion Channels, the atomic structure is so complex that direct summation of vdW forces is tedious, instead a dielectric function approach is desired

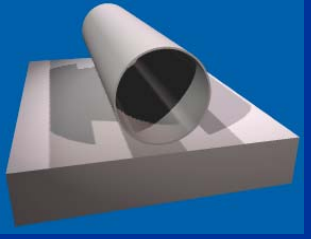

Fluctuation Forces

- **Fluctuation forces arise when the mean of the interaction =0 i.e. between neutral atoms /J.D.van der Waals, 1873/ or quantum systems in the ground state /F. London, 1930/**

$$V = -p_1 E(r_1) - p_2 E(r_2)$$

$$\langle p \rangle = 0$$

$$\langle p^2 \rangle \neq 0$$

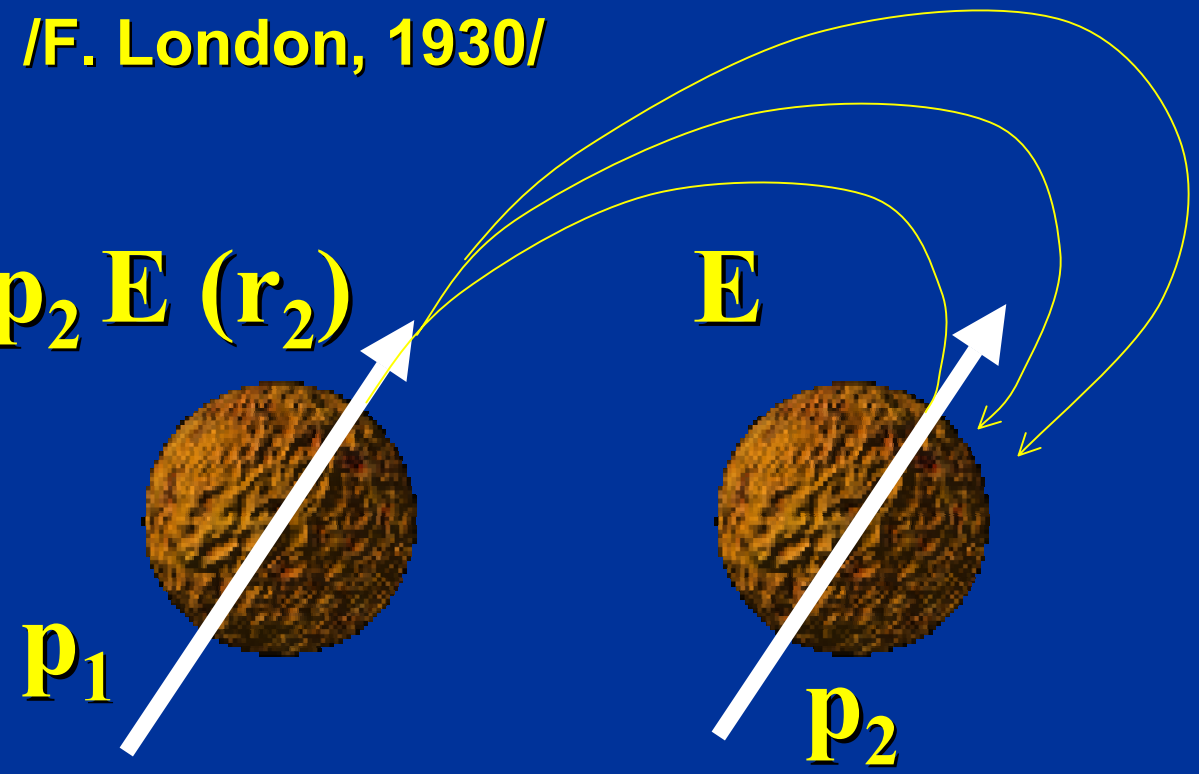

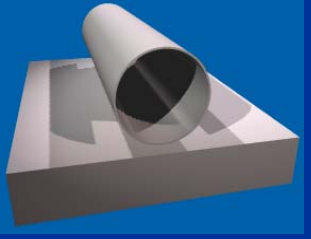

vdW potential: Is it 6-12

- Attraction follows to the Electrodynamics
- Repulsion, which is due to Pauli principle, is a short-range potential:

any rational fit works (12, 18, 100, exp, even “hard-wall”)

- Dimensional analysis for 0D (an atom) interacting with e/m vacuum modes - exclusion principle: volume of metal sphere ~ R_1^3

$$V \sim - V_c \; R_1^3 R_2^3 / L^6$$

Adapted from J.Feinberg et.al., RMP 2001

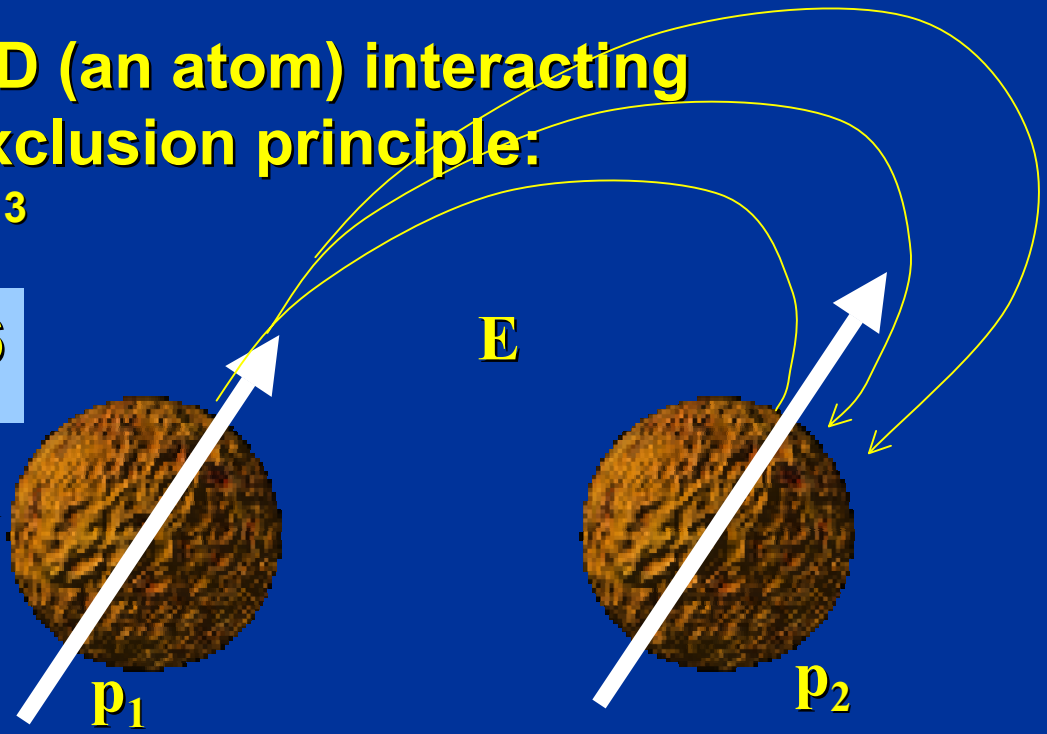

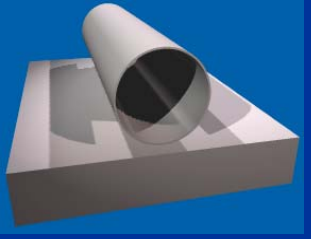

Fluctuation Forces (2)

$$V \sim - V_c \; R_1^3 R_2^3 / L^6$$

$V_c \sim kT$ - thermal fluctuations

$V_c \sim ck_c \sim hc/L$ - retarded fluctuations

$V_c \sim \hbar\omega_o$ - quantum fluctuations ⇒ vdW forces

Thermal fluctuations are weak and develop at micro-scale:

$$L_T \sim hc/kT \sim 1\mu m$$

Retarded fluctuations are less important at nano-scale distances:

$$c\hbar\omega \sim c/\omega_o \sim L_{Casimir} > 10nm$$

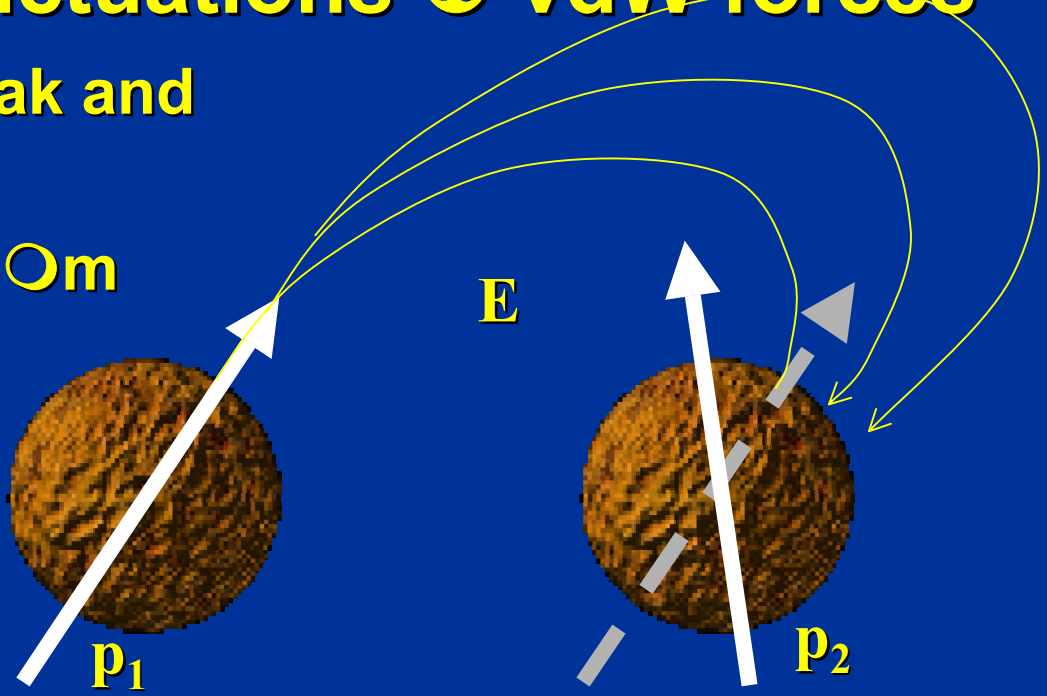

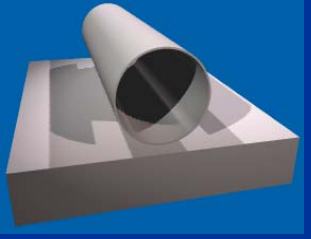

Van der Waals forces: what we expect

- **vdW forces, in general, are believed to be**
  - **<u>weak</u>** owing to a characteristic length R_1, $R_2 \sim a_B \ll D$
    so even if characteristic energy $V_c \sim IP \sim E_B$: $(a_B/D)^6 \ll 1$
  - **<u>short ranged</u>** if potential $\sim r^{-d}$ then for two solid bodies a total energy $\sim r^{-(d-6)}$: $d_c=6$
  - **<u>not specific</u> to a system** a substance defines only characteristic energy
  - **almost <u>one-body</u>** allowed 3-site corrections are tiny

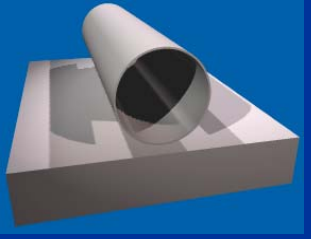

Van der Waals forces: what happens for NTs

- **In NT systems, on contrary, vdW forces are**
  - **strong** due to device length scale ~nm or ~Angstroms
  - **range for device operation is also (sub-) nm**
  - **specific to a system** characteristic energy ~ ~ frequency of specific 1D/2D mode
    - 2D specifics owing to shell structure in layered materials
    - 1D specifics owing to axial symmetry of considered systems
  - **many-body** collective (delocalized) excitations are important due to large oscillator strengths

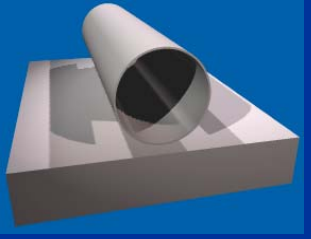

Details of Computation

- **vdW energy as a change of the total energy of Local Electromagnetic Modes**

$$H_o = \sum_{k,\mu} \hbar\omega_{k\mu}\left(n_{k\mu} + \frac{1}{2}\right)$$

$$\omega_{k\mu} = \omega_p \sqrt{R^2\left(k^2 + \frac{\mu^2}{R^2}\right) K_\mu(kR) I_\mu(kR)}$$

where 2D plasmon frequency $\omega_p = \sqrt{\dfrac{4\pi n e^2}{mR}}$

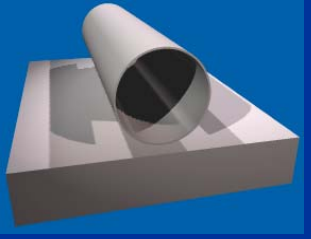

Details of Computation

- **Semiclassical approach for interacting plasmons**

$$\begin{cases} \dfrac{\partial j}{\partial t} = -\dfrac{ne^2}{m}\nabla\varphi \\ \\ \dfrac{\partial \sigma}{\partial t} + \nabla j = 0 \end{cases} \qquad n = \frac{16}{3\sqrt{3}b^2}$$

$$4\pi\sigma_{k\mu} = \varphi_{k\mu}\,\frac{1}{RK_\mu(kR)I_\mu(kR)}$$

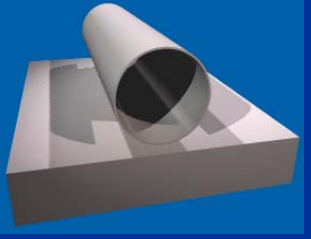

Details of Computation

- **Interacting plasmons change its zero-point oscillation energy: the Lagrangian of Interaction**

$$L = \frac{1}{2}\sum_{k,\mu}\left(\frac{\omega^2}{\omega^2_{k\mu}(1)} - 1\right)\sigma^{\dagger}_{k\mu}(1)\varphi_{k\mu}(1) + \frac{1}{2}\sum_{K,M}\left(\frac{\omega^2}{\omega^2_{KM}(2)} - 1\right)\sigma^{\dagger}_{KM}(2)\varphi_{KM}(2) -$$

$$\frac{1}{2}\sum_{k,\mu;K,M} V(1-2)\left(\sigma^{\dagger}_{k\mu}(1)\varphi_{KM}(2) + \sigma^{\dagger}_{KM}(2)\varphi_{k\mu}(1)\right) + h.c.$$

- **Secular equation for plasmon frequency for tube-to-tube and tube-to-substrate interactions**

$$\sqrt{\left(-\frac{\omega^2}{\omega^2_{k\mu}(1)} + 1\right)\left(-\frac{\omega^2}{\omega^2_{k\mu}(2)} + \frac{K_\mu(kR_2)I_\mu(kR_2)}{K_\mu(kR_1)I_\mu(kR_1)}\right)} = \mp\frac{I_\mu(kR_2)K_{2\mu}(kD)}{K_\mu(kR_1)}$$

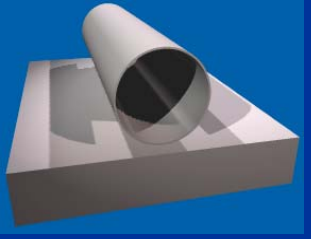

Details of Computation

- **Secular equation for plasmon frequency for tube-to-tube and tube-to-substrate interactions**

$$\begin{vmatrix} -\dfrac{\omega^2}{\omega_{k\mu}^2(1)} + 1 & \dfrac{I_\mu(kR_2)K_{2\mu}(kD)}{K_\mu(kR_1)} \\ \dfrac{I_\mu(kR_2)K_{2\mu}(kD)}{K_\mu(kR_1)} & -\dfrac{\omega^2}{\omega_{k\mu}^2(2)} + \dfrac{K_\mu(kR_2)I_\mu(kR_2)}{K_\mu(kR_1)I_\mu(kR_1)} \end{vmatrix} = 0$$

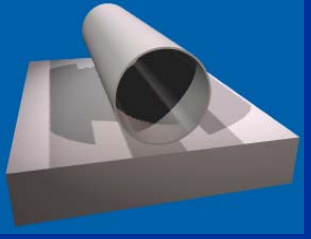

Tube-Tube interaction

- **Many-body term has a fractional power law for distance dependence due to 1D character of plasmons**

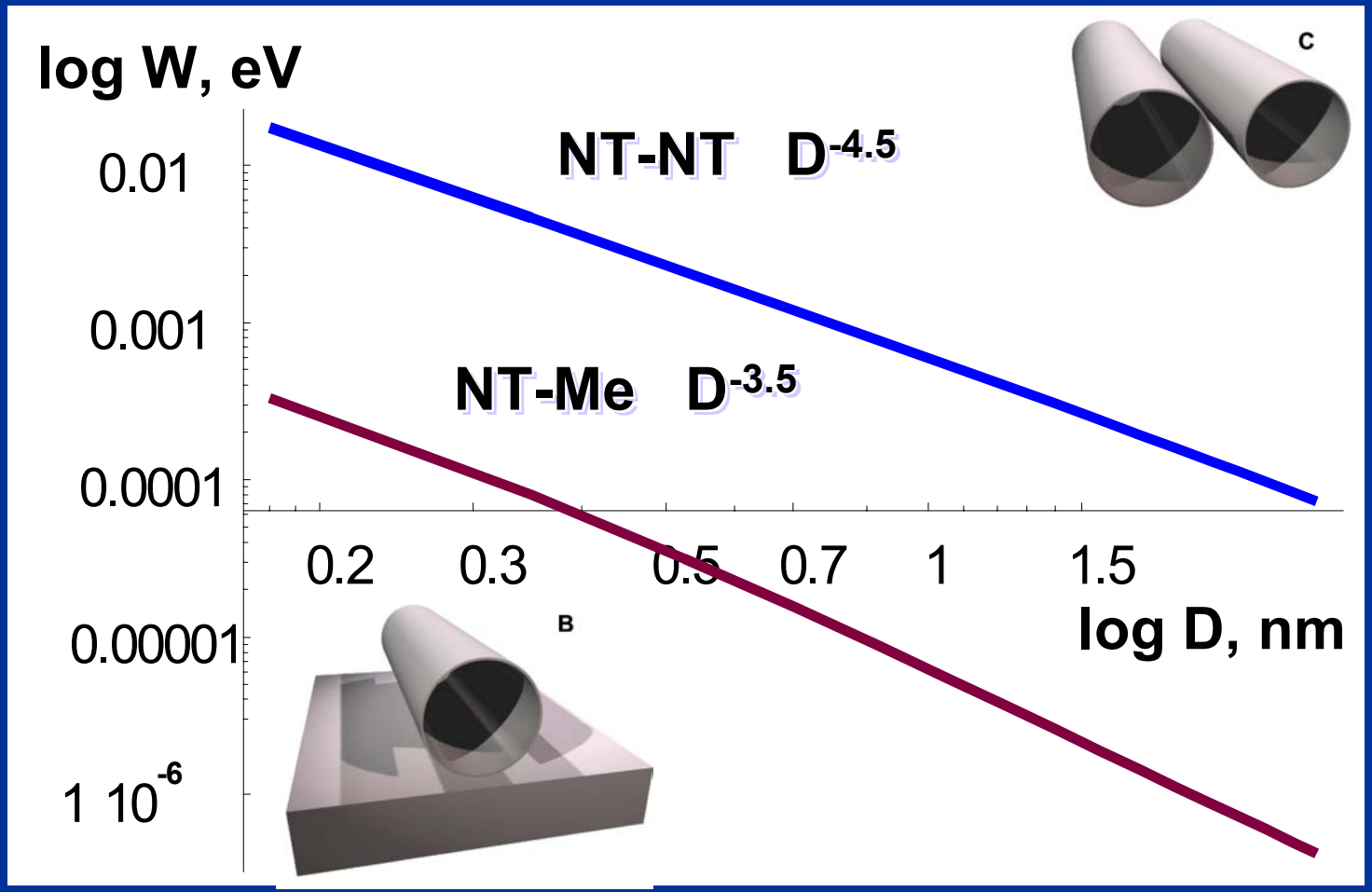

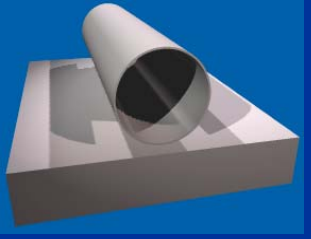

Details of Computation

- **Starting with the same Lagrangian of Interaction we can compute almost any axial shell system**

$$L = \frac{1}{2}\sum_{k,\mu}\left(\frac{\omega^2}{\omega^2_{k\mu}(1)} - 1\right)\sigma^{\dagger}_{k\mu}(1)\varphi_{k\mu}(1) + \frac{1}{2}\sum_{K,M}\left(\frac{\omega^2}{\omega^2_{KM}(2)} - 1\right)\sigma^{\dagger}_{KM}(2)\varphi_{KM}(2) -$$

$$\frac{1}{2}\sum_{k,\mu;K,M} V(1-2)\left(\sigma^{\dagger}_{k\mu}(1)\varphi_{KM}(2) + \sigma^{\dagger}_{KM}(2)\varphi_{k\mu}(1)\right) + h.c.$$

- **For example, here is secular equation for plasmon frequency for intershell interactions in DWNT**

$$\sqrt{\left(-\frac{\omega^2}{\omega^2_{k\mu}(1)} + 1\right)\left(-\frac{\omega^2}{\omega^2_{k\mu}(2)} + \frac{K_\mu(kR_2)I_\mu(kR_2)}{K_\mu(kR_1)I_\mu(kR_1)}\right)} = \mp\frac{K_\mu(kR_2)}{K_\mu(kR_1)}$$

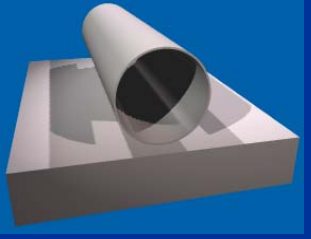

Details of Computation

- **Secular equation for plasmon frequency for intershell interactions in DWNT**

$$\begin{vmatrix} -\dfrac{\omega^2}{\omega_{k\mu}^2(1)} + 1 & \dfrac{K_\mu(kR_2)}{K_\mu(kR_1)} \\ \dfrac{K_\mu(kR_2)}{K_\mu(kR_1)} & -\dfrac{\omega^2}{\omega_{k\mu}^2(2)} + \dfrac{K_\mu(kR_2)I_\mu(kR_2)}{K_\mu(kR_1)I_\mu(kR_1)} \end{vmatrix} = 0$$

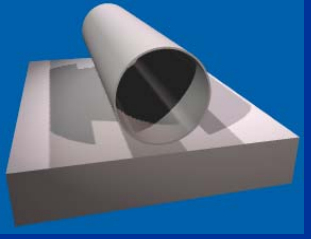

Interaction between walls

- Inter-wall interaction in DWNT decays as ~$D^{2.6}$

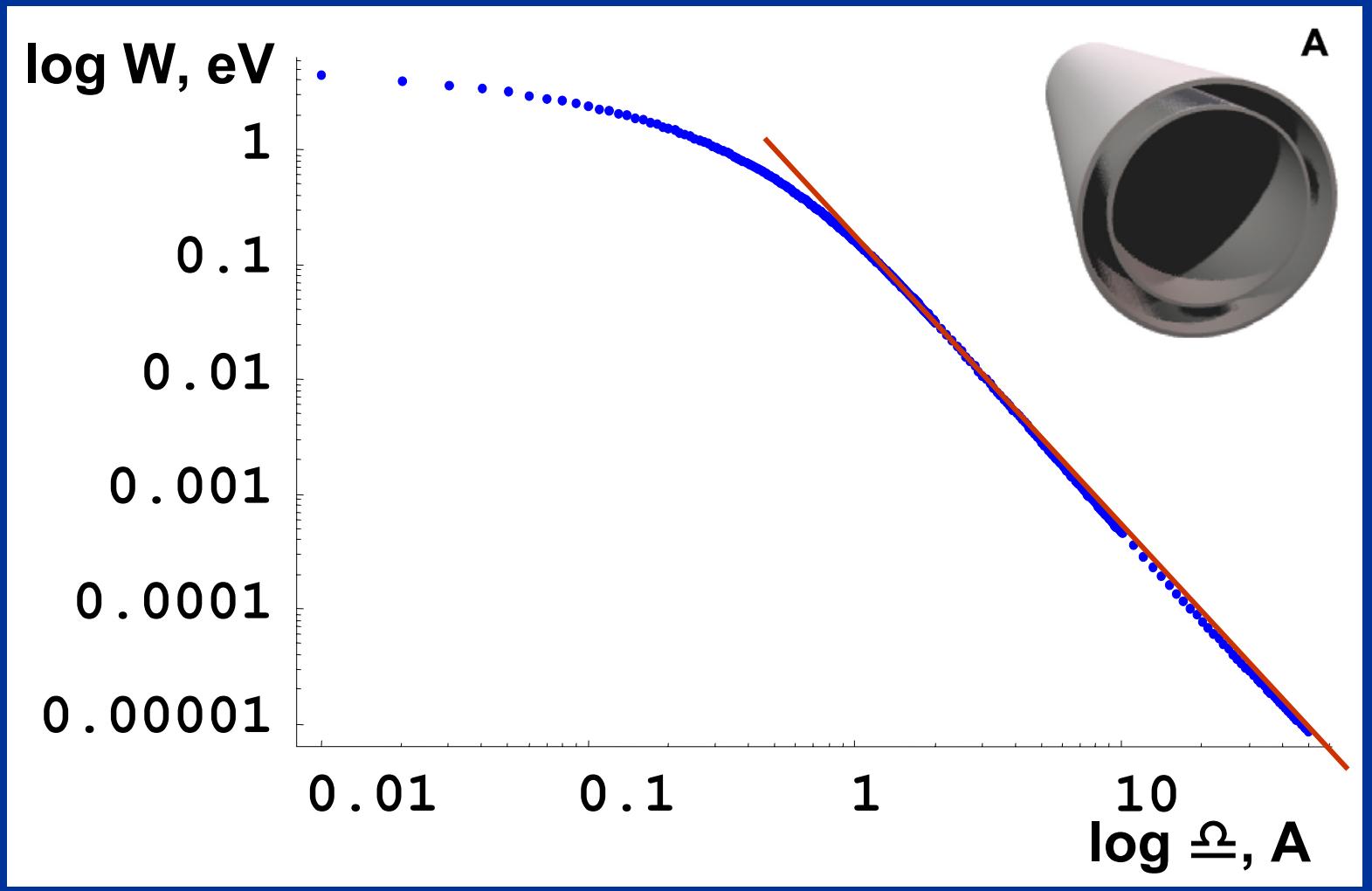

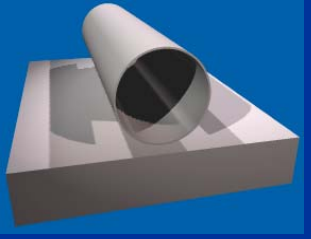

Inter-wall vdW interaction in real carbon NT structures

- Formation of peapods (C_{60} intercalated SWNTs)
- Formation of DWNTs from peapods
  - D. Luzzi et. al. (2000)
  - S. Iijima et. al. (2000, 2001)

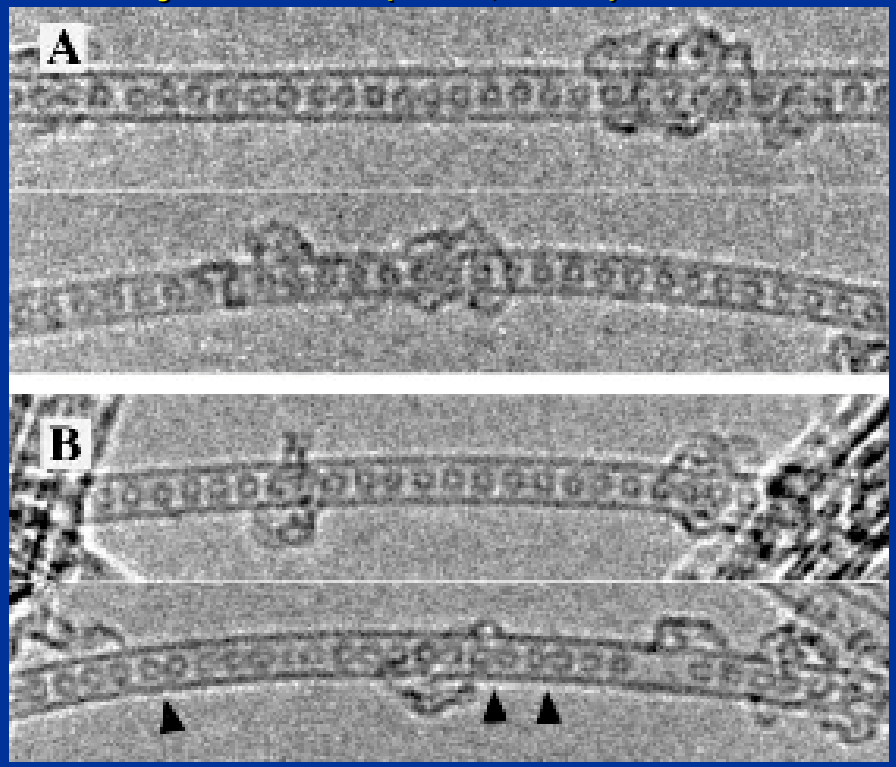

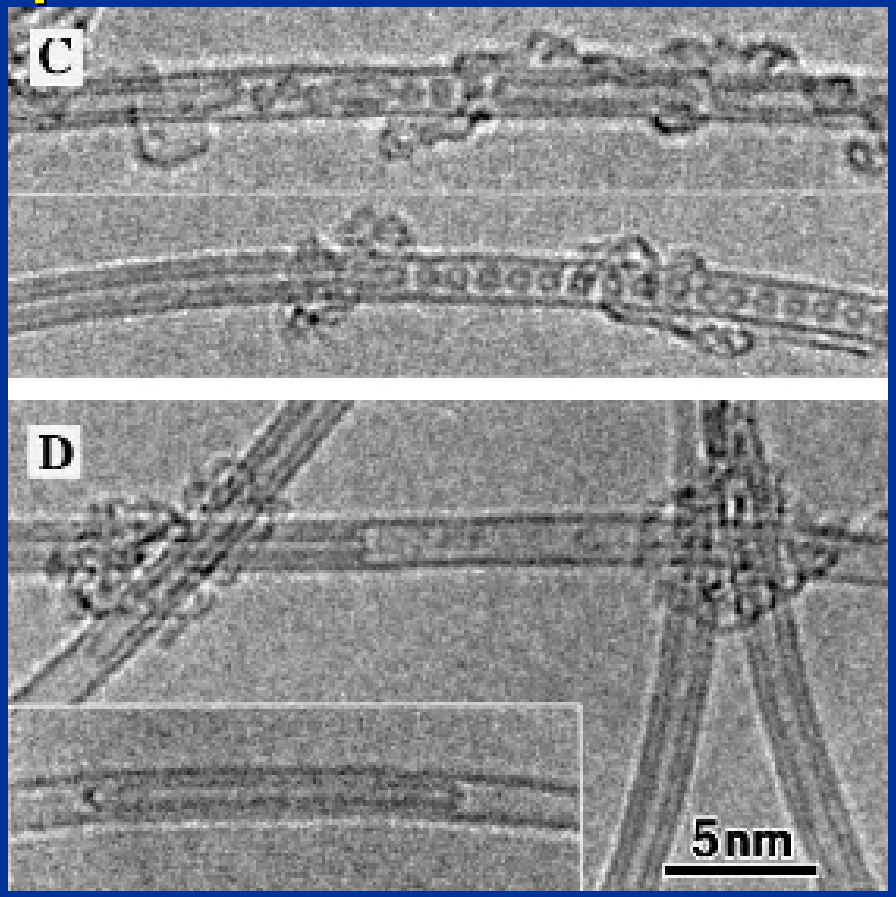

STS image of SWNT peapods

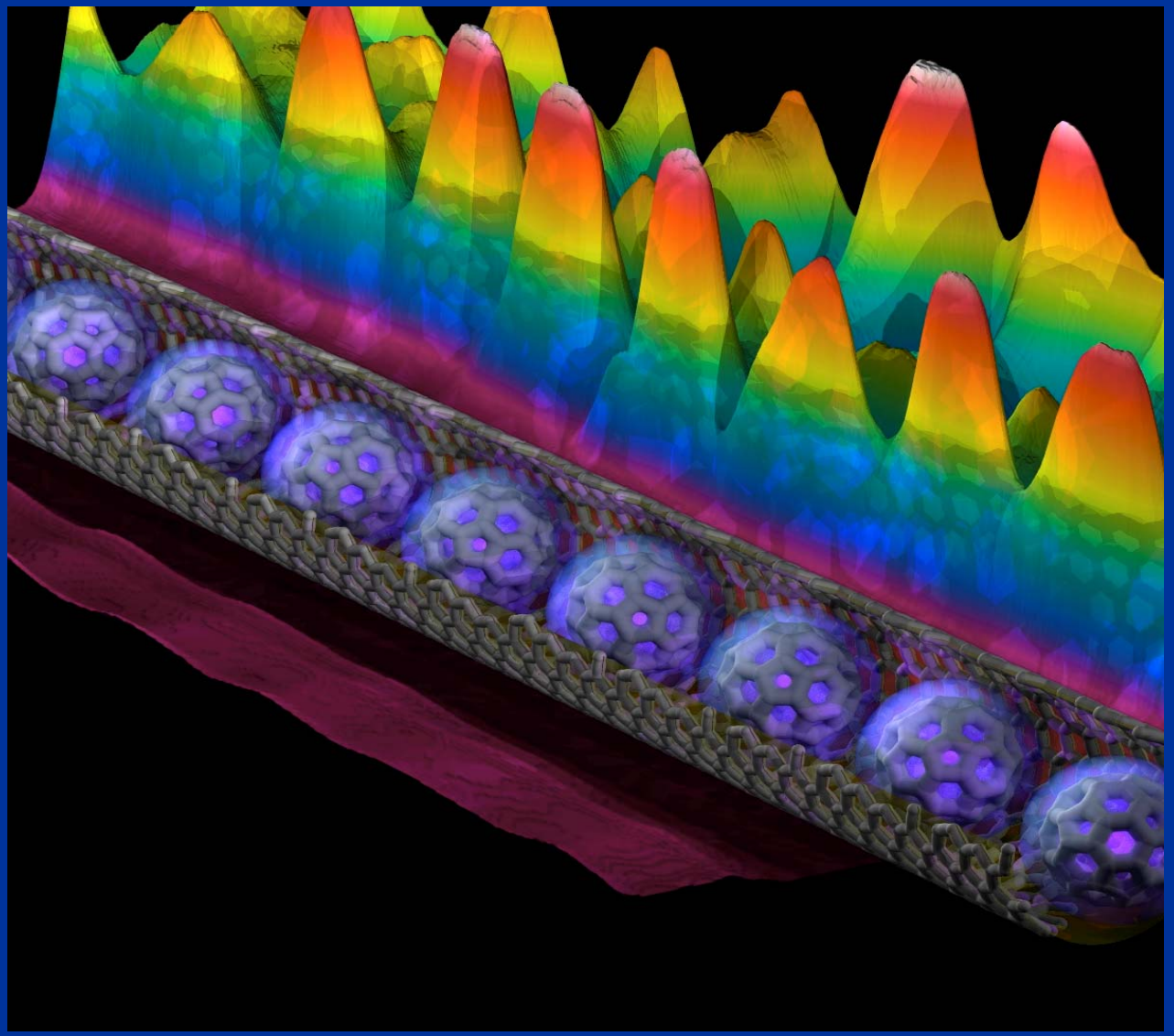

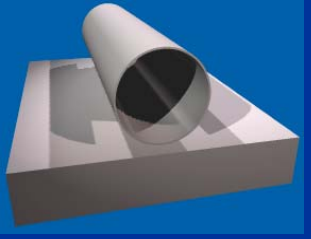

Toward Modeling of Device

- NEMS applications of nanotubes are expected to follow recent progress in the NT fabrication

Experimental realization: growth on silicide islands

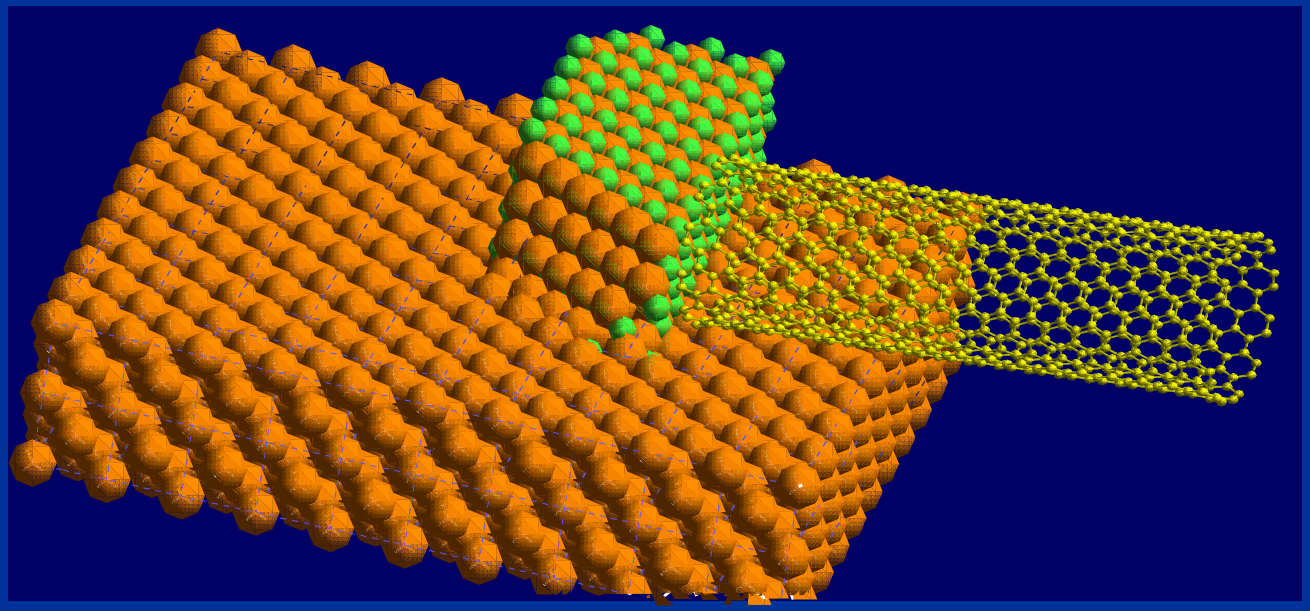

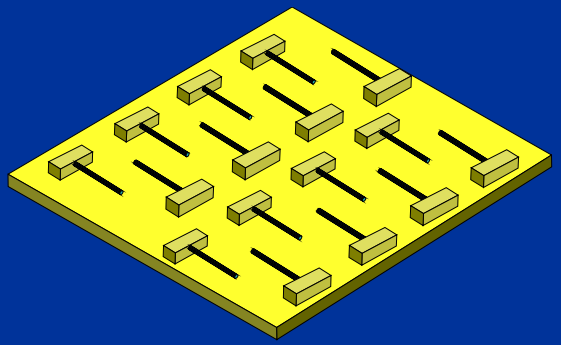

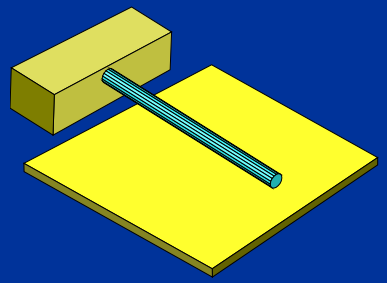

- NT on chip: a future technology

Conclusions

- A Compact Continuum Model for simulation of Carbon Nanotube Devices has been developed:
  - continuum methods have been elaborated and verified with the use of Quantum and Molecular Mechanics
  - attractive part of van der Waals force was computed
  - electrostatics of NT based systems is developed
  - electronic structure was simulated at equilibrium
- Theory of NT Devices is essentially non-classical
- Atomistic (quantum) effects were studied
- Future directions for the simulation:
  - other Transport Devices: NT-Switch, NT-FET, NT-Diode
  - higher level of integration
  - microscopics of non-ideal systems

Acknowledgements

Thanks to experimentalists and theoreticians who stimulated this work:

- Prof. Karl Hess (UIUC),
- Prof. Narayan R. Aluru (UIUC),
- Prof. Joe Lyding (UIUC),
- Prof. Yuri Gogotsi (Drexel),
- Prof. Michel Barsoum (Drexel),
- Prof. Jean-Pierre Leburton (UIUC),
- Prof. Alex Shik (ECAN, Toronto),
- Mr. Kirill A. Bulashevich (StPTU)
- Dr. Lolita Rotkina (UIUC),
- Dr. Ilya Zharov (UIUC),
- Dr. Alexey G. Petrov (Ioffe),
- Mr. Marc Dequesnes (UIUC),
- Prof. Scott Carney (UIUC),
- Prof. Alexey Bezryadin (UIUC),
- Prof. Richard Martin (UIUC),
- Prof. Robert A. Suris (Ioffe)

New students are welcome

New students are welcome

Support from CRI grant of UIUC, DoE grant and Arnold and Mabel Beckman Foundation

Overview